Cell Metabolism
Clinical and Translational Report

Early downmodulation of tumor glycolysis predicts response to fasting-mimicking diet in triple-negative breast cancer patients

Graphical abstract

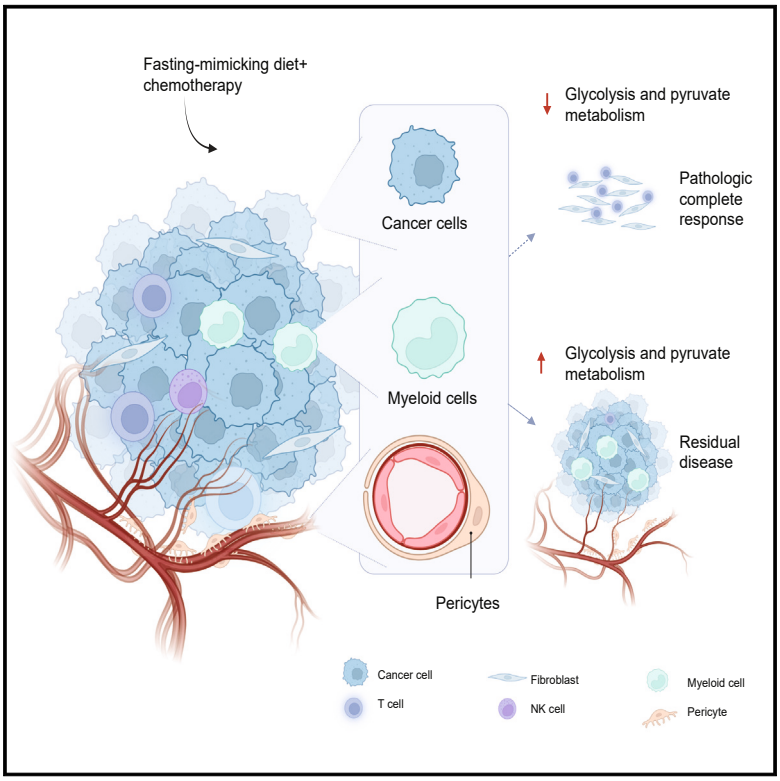

Highlights

- Cyclic FMD plus anthracycline-taxane CT resulted in excellent responses in early TNBC
- The experimental treatment was safe, and patient compliance was excellent
- Early downmodulation of glucose metabolism in cancer cells predicts pCR to FMD

Authors

Francesca Ligorio, Andrea Vingiani, Tommaso Torelli, ..., Giancarlo Pruneri, Filippo de Braud, Claudio Vernieri

Correspondence

claudio.vernieri@istitutotumori.mi.it

In brief

In brief, Vernieri et al. conducted a pilot, randomized phase 2 trial showing that cyclic FMD plus preoperative chemotherapy results in excellent pCR rates in stage I–III TNBC patients. In tumors achieving pCR, bulk and single-cell RNA-seq analysis revealed early downmodulation of glucose metabolism in TNBC cells and in glycolytic intratumor cells.

Ligorio et al., 2025, Cell Metabolism *37*, 330–344
February 4, 2025
https://doi.org/10.1016/j.cmet.2024.11.004

CellPress

CellPress

Cell Metabolism

Clinical and Translational Report

Early downmodulation of tumor glycolysis predicts response to fasting-mimicking diet in triple-negative breast cancer patients

Francesca Ligorio,[1,2,14] Andrea Vingiani,[3,4,14] Tommaso Torelli,[4] Caterina Sposetti,[1,3] Lorenzo Drufuca,[2] Fabio Iannelli,[5] Lucrezia Zanenga,[1] Catherine Depretto,[6] Secondo Folli,[7] Gianfranco Scaperrotta,[6] Giuseppe Capri,[1] Giulia V. Bianchi,[1] Cristina Ferraris,[7] Gabriele Martelli,[7] Ilaria Maugeri,[7] Leonardo Provenzano,[1,3] Federico Nichetti,[1] Luca Agnelli,[4] Riccardo Lobefaro,[1] Giovanni Fucà,[1] Giuseppe Fotia,[1] Luigi Mariani,[8] Daniele Morelli,[4] Vito Ladisa,[9] Maria Carmen De Santis,[6] Laura Lozza,[6] Giovanna Trecate,[6] Antonino Belfiore,[4] Silvia Brich,[4] Alessia Bertolotti,[4] Daniele Lorenzini,[3,4] Angela Ficchì,[1] Antonia Martinetti,[1] Elisa Sottotetti,[1] Alessio Arata,[1] Paola Corsetto,[10] Luca Sorrentino,[7] Mattia Rediti,[2] Giulia Salvadori,[2] Saverio Minucci,[3,11] Marco Foiani,[2,3] Giovanni Apolone,[12] Massimiliano Pagani,[2,13] Giancarlo Pruneri,[3,4,15] Filippo de Braud,[1,3,15] and Claudio Vernieri[1,2,15,16,*]

[1]Medical Oncology Department, Fondazione IRCCS Istituto Nazionale dei Tumori, Via Venezian 1, 20133 Milan, Italy
[2]IFOM ETS, the AIRC Institute of Molecular Oncology, Via Adamello 16, 20139 Milan, Italy
[3]Oncology and Hematology-Oncology Department, University of Milan, Via Festa del Perdono 7, 20122 Milano, Italy
[4]Department of Advanced Diagnostics, Fondazione IRCCS Istituto Nazionale dei Tumori, Via Venezian 1, 20133 Milan, Italy
[5]Haematopathogy Division, IEO, European Institute of Oncology IRCCS, Via Ripamonti 435, 20141 Milan, Italy
[6]Department of Radiology and Radiotherapy, Fondazione IRCCS Istituto Nazionale dei Tumori, Via Venezian 1, 20133 Milan, Italy
[7]Surgical Oncology Department, Fondazione IRCCS Istituto Nazionale dei Tumori, Via Venezian 1, 20133 Milan, Italy
[8]Unit of Clinical Epidemiology and Trial Organization, Fondazione IRCCS Istituto Nazionale dei Tumori, Via Venezian 1, 20133 Milan, Italy
[9]Hospital Pharmacy, Fondazione IRCCS Istituto Nazionale dei Tumori, Via Venezian 1, 20133 Milan, Italy
[10]Department of Pharmacological and Biomolecular Sciences, University of Milan, Via Festa del Perdono 7, 20122 Milan, Italy
[11]Department of Experimental Oncology, IEO, European Institute of Oncology IRCCS, Via Adamello 16, 20139 Milan, Italy
[12]Scientific Directorate, Fondazione IRCCS Istituto Nazionale dei Tumori, Via Venezian 1, 20133 Milan, Italy
[13]Department of Medical Biotechnology and Translational Medicine, University of Milan, Via Festa del Perdono 7, 20122 Milan, Italy
[14]These authors contributed equally
[15]Senior author
[16]Lead contact
*Correspondence: claudio.vernieri@istitutotumori.mi.it
https://doi.org/10.1016/j.cmet.2024.11.004

SUMMARY

In preclinical experiments, cyclic fasting-mimicking diets (FMDs) showed broad anticancer effects in combination with chemotherapy. Among different tumor types, triple-negative breast cancer (TNBC) is exquisitely sensitive to FMD. However, the antitumor activity and efficacy of cyclic FMD in TNBC patients remain unclear. Here, we show that a severely calorie-restricted, triweekly, 5-day FMD regimen results in excellent pathologic complete response (pCR) rates (primary endpoint) and long-term clinical outcomes (secondary endpoints) when combined with preoperative chemotherapy in 30 patients with early-stage TNBC enrolled in the phase 2 trial BREAKFAST. Bulk and single-cell RNA sequencing analysis revealed that highly glycolytic cancer cells, myeloid cells, and pericytes from tumors achieving pCR undergo a significant, early downmodulation of pathways related to glycolysis and pyruvate metabolism. Our findings pave the wave for conducting larger clinical trials to investigate the efficacy of cyclic FMD in early-stage TNBC patients and to validate early changes of intratumor glycolysis as a predictor of clinical benefit from nutrient restriction. This study was registered at Clinicaltrials.gov (NCT04248998).

INTRODUCTION

In the last two decades, nutrient restriction approaches, such as cyclic fasting or fasting-mimicking diets (FMDs), consistently showed broad anticancer effects in preclinical tumor models,[1–9] and they synergized with chemotherapy, immunotherapy, endocrine, or targeted therapies to slow down *in vivo* tumor growth, to prolong animal survival, and to increase animal cure rates.[1–5,8–10] The *in vivo* antineoplastic effects of fasting/FMDs can be attributed to a combination of metabolic changes that affect crucial biological processes in cancer cells and the functional status of tumor-infiltrating immune cells.[1–3,8,10]

Recently, our group demonstrated that a severely calorie-restricted, low-carbohydrate, low-protein, 5-day FMD regimen

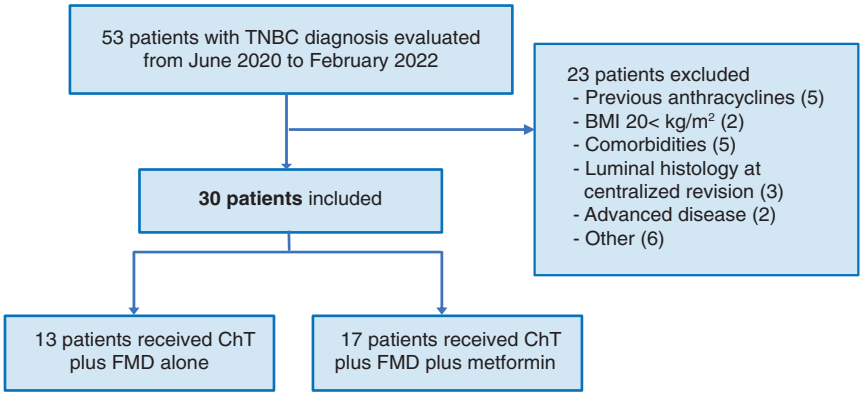

Figure 1. CONSORT diagram

Between June 2020 and February 2022, *n* = 53 patients with newly diagnosed stage I–III TNBC were evaluated. After excluding patients not fulfilling inclusions and exclusions criteria, *n* = 30 patients were enrolled in the BREAKFAST trial, 13 of whom were randomized to arm A and 17 to arm B. ChT, chemotherapy; BMI, body mass index; FMD, fasting-mimicking diet; TNBC, triple-negative breast cancer.

is safe and well tolerated when combined with standard anticancer therapies in patients with different tumor types, and it results in desirable metabolic and immunological modifications that recapitulate the biological effects responsible for the antineoplastic activity of nutrient starvation in preclinical experiments.[11] In this study, a few patients with advanced malignancies, such as triple-negative breast cancer (TNBC), pancreatic, colorectal, or lung carcinoma, achieved complete and long-lasting tumor remissions when cyclic FMD was combined with standard systemic treatments.[12,13] Albeit interesting, these anecdotal responses do not provide clinically meaningful evidence of antitumor activity or efficacy of cyclic FMD in combination with standard treatments in specific clinical contexts.

Among different tumor types, TNBC is exquisitely sensitive to glucose deprivation.[1–3,9,10] In TNBC-bearing mice, cyclic FMD inhibited the cancer stem cell (CSC) compartment and contributed to activate tumor-infiltrating T lymphocytes, thus resulting in cooperative antitumor effects in combination with phosphatidylinositol 3-kinase (PI3K)/AKT/mTORC1 axis inhibitors and with immune checkpoint inhibitors.[1,2,9] More recently, combining glucose restriction with the antidiabetic compound metformin caused synergistic antitumor effects in several *in vitro* and *in vivo* tumor models through the concomitant inhibition of glycolysis and mitochondrial oxidative phosphorylation (OXPHOS), thus preventing tumor cells' metabolic adaptation to fasting.[14]

Based on strong preclinical rationale, the pilot, phase2 randomized trial BREAKFAST (NCT04248998) investigated whether combining cyclic FMD with preoperative anthracycline-cyclophosphamide-taxane chemotherapy, plus or minus metformin, increases pathologic complete response (pCR) rates in patients with early-stage TNBC when compared with preoperative chemotherapy alone according to historical data (Figure S1). We combined bulk and single-cell tumor transcriptomics with body composition analyses to identify potential biomarkers of tumor response to the experimental treatment.

RESULTS

Cyclic FMD is safe in combination with chemotherapy plus/minus metformin

Patient enrollment initiated in June 2020, and it was precociously interrupted in February 2022, when the results of the KEYNOTE 522 trial established chemoimmunotherapy as the new, standard-of-care neoadjuvant treatment for stage-II and III TNBC patients.[15,16] Between June 2020 and February 2022, we enrolled 30 patients, 13 of whom were randomized to arm A (without metformin) and 17 to arm B (with metformin) (Figure 1). Patient and tumor characteristics were equally distributed in the two treatment arms (Table 1).

The incidence of severe adverse events (AEs) (grade 3 or grade 4) was 70%. Severe AEs attributable to the FMD and serious AEs (SAEs) occurred in 3% and 6.7% of all patients, respectively, with all SAEs consisting of febrile neutropenia events (12% of the patients in arm B, and none of the patients in arm A) (Table S1). Any grade diarrhea was more common in patients receiving metformin (arm B vs. arm A: 71% vs. 31%, respectively, $p = 0.03$), whereas other AEs were similarly distributed in the two treatment arms (Table S1). No patients experienced significant left ventricle ejection fraction (LVEF) decline during anthracycline-based chemotherapy (Figure S2A), similarly to what was observed in an independent retrospective, control (CTRL) cohort of 33 TNBC patients treated with anthracyclines-based chemotherapy without FMD at our institution (Figures S2B and S2C).

The majority (*n* = 22; 73.3%) of patients were able to successfully complete the maximum number of FMD cycles allowed as per protocol (*n* = 8) (Figure S2D). Regarding adherence to the FMD, 19 (63.3%) patients were fully compliant during each FMD cycle, and 88.9% of all FMD cycles were successfully completed without major or minor deviations (Figure S2E). Patient adherence to the FMD was not affected by concomitant metformin use (chi-squared test $p = 0.35$).

The most common cause of precocious FMD discontinuation (7 out of 8 patients) was patient inability to restore a minimum body mass index (BMI) of 20 kg/m^2 before the subsequent FMD cycle, while only one patient interrupted the FMD because of the occurrence of grade-2 fatigue. In arm B patients, metformin was overall very well tolerated, with only 4 patients (23.5%) requiring a dose reduction and 2 patients (11.8%) discontinuing metformin (*n* = 1 for liver toxicity and *n* = 1 for weight loss).

Cyclic FMD in combination with chemotherapy is active in TNBC patients

All patients enrolled in the BREAKFAST trial were able to complete the neoadjuvant pharmacologic treatment before undergoing surgery. The pCR rate was 56.6% in the whole study cohort, and it was not significantly different in arm A vs. arm B patients (7/13, 53.9% vs. 10/17, 58.8%, respectively; odds ratio [OR]

Table 1. Patient characteristics

Characteristic	Overall (*n* = 30)	Arm A (*n* = 13)	Arm B (*n* = 17)	*p* value
Age				
Median (IQR)	50.2 (46.9–56.2)	50.9 (47.3–54.1)	49.6 (46.8–57.9)	0.691[a]
Menopausal status				
Post-menopausal	17 (56.7)	5 (38.5)	12 (70.6)	0.165
Pre-menopausal	13 (43.3)	8 (61.5)	5 (29.4)	–
Grade				
2	1 (3.3)	1 (7.7)	0 (0.0)	0.891
3	29 (96.7)	12 (92.3)	17 (100.0)	–
Ki67				
Median (IQR)	61.5 (36.8–83.8)	60.0 (27.0–85.0)	63.0 (45.0–80.0)	0.438
HER2 status (IHC)				
0	16 (53.3)	6 (46.2)	10 (58.8)	0.240
1+	12 (40.0)	5 (38.5)	7 (41.2)	–
2+	2 (6.7)	2 (15.4)	0 (0.0)	–
TILs				
Median (IQR)	20.0 (8.0–30.0)	20.0 (8.0–26.0)	21.5 (8.8–31.2)	0.843
High (>20)	13 (44.8)	5 (38.5)	8 (50.0)	0.806
Low (≤20)	16 (55.2)	8 (61.5)	8 (50.0)	–
Primary tumor				
T1c	8 (26.7)	4 (30.8)	4 (23.5)	0.812
T2	19 (63.3)	8 (61.5)	11 (64.7)	–
T3	1 (3.3)	0	1 (5.9)	–
T4	2 (6.7)	1 (7.7)	1 (5.9)	–
Nodal involvement				
N0	21 (70.0)	8 (61.5)	13 (76.5)	0.526
N1	5 (16.7)	3 (23.1)	2 (11.8)	–
N2	1 (3.3)	0 (0.0)	1 (5.9)	–
N3	3 (10.0)	2 (15.4)	1 (5.9)	–
Stage				
Stage I	4 (13.3)	1 (7.7)	3 (17.6)	0.712
Stage II	20 (66.7)	9 (69.2)	11 (64.7)	–
Stage III	6 (20.0)	3 (23.1)	3 (17.6)	–
Type of surgery				
BCS	13 (43.3)	6 (46.2)	7 (41.2)	1.000
Mastectomy	17 (56.7)	7 (53.8)	10 (58.8)	–
Germline mutations				
BRCA1	7 (23%)	3 (23%)	4 (24%)	0.8
PALB2	1 (3.3%)	1 (7.7%)	0 (0%)	–
WT	15 (50%)	7 (54%)	8 (47%)	–
Not performed	7 (23%)	2 (15%)	5 (29%)	–
BMI				
Median (IQR)	23.8 (21.5–26.7)	23.1 (22.5–27.5)	24.0 (21.1–25.6)	0.517[a]

Data are presented as *n* (%) except where otherwise noted. The *p* value of the Pearson's chi-squared test assessing the association between each characteristic and treatment arm is indicated in the right column of the table, except where otherwise noted. The *p* value of the test is indicated in bold numbers when statistically significant. *p* values were calculated excluding unknown values. BMI, body mass index; IHC, immunohistochemistry; IQR, interquartile range; BCS, breast-conserving surgery; WT, wild type; TILs, tumor-infiltrating lymphocytes.
[a]Wilcoxon rank-sum test.

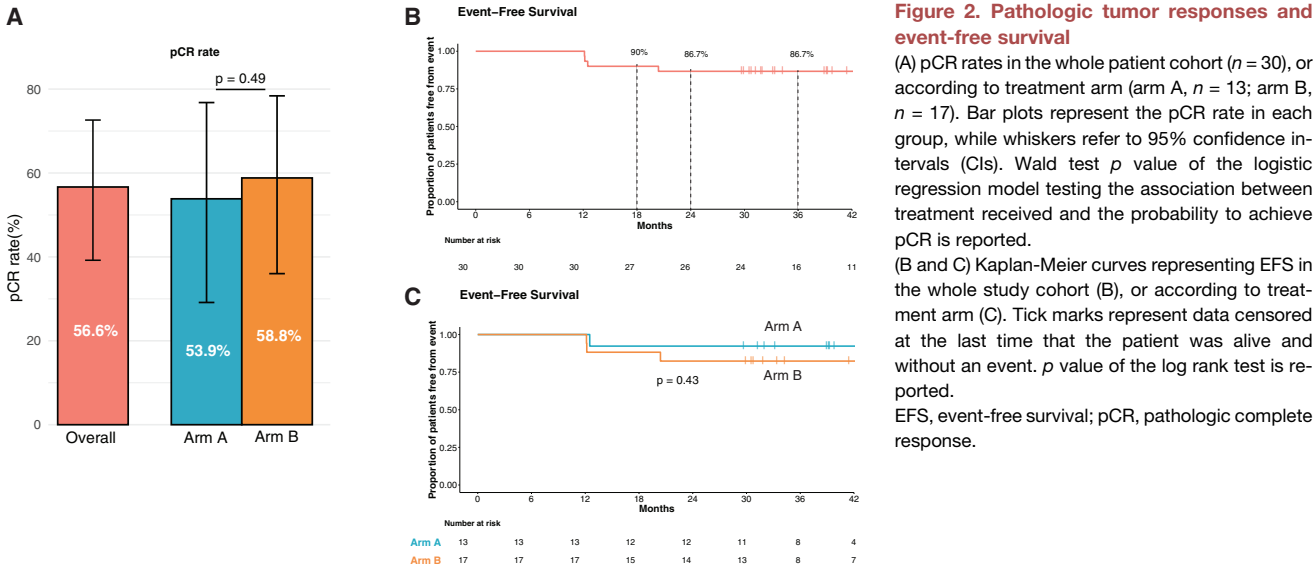

Figure 2. Pathologic tumor responses and event-free survival

(A) pCR rates in the whole patient cohort ($n = 30$), or according to treatment arm (arm A, $n = 13$; arm B, $n = 17$). Bar plots represent the pCR rate in each group, while whiskers refer to 95% confidence intervals (CIs). Wald test p value of the logistic regression model testing the association between treatment received and the probability to achieve pCR is reported.

(B and C) Kaplan-Meier curves representing EFS in the whole study cohort (B), or according to treatment arm (C). Tick marks represent data censored at the last time that the patient was alive and without an event. p value of the log rank test is reported.

EFS, event-free survival; pCR, pathologic complete response.

1.67, 95% confidence interval [CI] 0.39–7.43, $p = 0.49$) (Figure 2A). Since the BREAKFAST trial did not include a CTRL arm of patients receiving chemotherapy alone, we compared the pCR rate observed in our study with tumor pCR rates previously reported in studies employing similar neoadjuvant chemotherapy regimens in early-stage TNBC patients,[17–23] as well as in an independent retrospective cohort of early-stage TNBC patients treated with neoadjuvant anthracycline-cyclophosphamide-taxane chemotherapy in our Institute (INT 92/20 study).[24] As shown in Table S2, the characteristics of patients enrolled in the BREAKFAST trial were overall similar to the characteristics of patients included in these CTRL cohorts, with the only exception of a higher percentage of patients with node-negative disease (cN0) in the BREAKFAST trial when compared with these CTRL cohorts. However, several studies have shown that the pCR rates observed in early-stage TNBC patients undergoing neoadjuvant chemotherapy or chemoimmunotherapy are not significantly different in patients with N0 vs. N1 disease (33% vs. 29% in N0 vs. N1 disease, respectively, in the anthracycline-paclitaxel arm of the BRIGHTNESS trial[22]; 64.9% vs. 64.8% in N0 vs. N1 disease in the KEYNOTE-522 trial with chemoimmunotherapy[15]).

Notably, the pCR rate observed in the BREAKFAST trial was higher than the pCR rate reported in previous studies including TNBC patients treated with similar neoadjuvant anthracycline-taxane regimens (including dose-dense regimens) (Table S2). The broad range of pCR rates reported in these studies (14%–48.5%) could be attributable to the heterogeneity of patients or chemotherapy regimens, which ranged from low-efficacy triweekly paclitaxel-based regimens (pCR rate: 14%[21]) to intense dose-dense anthracycline-taxane chemotherapy, such as in the GeparOcto GBG84 trial (pCR rate: 48.5%[25]). When focusing on the three studies employing chemotherapy regimens similar to that used in the BREAKFAST trial, the reported pCR rate varied in the 30%–39% interval.[17,19,22]

With a median follow-up of 39.3 months, 4 tumor relapse events were detected (13.3%), with 18, 24, and 36 months event-free survival (EFS) rates of 90%, 86.7%, and 86.7%, respectively (Figure 2B). EFS was not statistically significantly different in the two treatment arms (Figure 2C). Similarly, promising results were observed in terms of relapse-free survival (RFS) and overall survival (OS) (Figures S3A and S3B). On the other hand, long-term clinical outcomes in 76 early-stage TNBC patients treated with anthracycline-taxane chemotherapy alone at our institution were worse than those reported in the BREAKFAST trial, with 3-year EFS and OS of 65.8% and 78.9%, respectively (Figures S3C and S3D).

FMD causes short- and long-term modifications of BMI and body composition

Patient BMI was significantly reduced after each FMD cycle, and it was almost, but not fully restored during the refeeding intervals, thus resulting in a significant BMI reduction after about 6 months of study treatment (Figure 3A). Patients who were overweight/obese at diagnosis (BMI $\geq$ 25 kg/m^2; Figure 3B) experienced a much more pronounced, long-term BMI reduction when compared with patients with a normal weight at baseline (median relative reduction: 11.3% vs. 3.7%, respectively, $p = 0.033$ (Figure 3B). Patient BMI was reduced during the study treatment regardless of pCR outcomes (Figure S4A). Although patients with high BMI at baseline had numerically higher probability to achieve pCR when compared with patients with normal BMI (72.7% vs. 47.4%, respectively; $p = 0.33$), this difference did not reach statistical significance, likely due to low patient numbers (Figure S4B). In the independent CTRL cohort of 76 early-stage TNBC patients treated with neoadjuvant chemotherapy alone at our institution, patient BMI was not modified during the course of neoadjuvant treatment (Figure S4C), neither in patients who had a normal weight at baseline, nor in those who were overweight or obese (Figure S4D). These data indicate that the reduction of BMI observed in patients enrolled in the BREAKFAST trial is likely to be attributable to the FMD (plus/minus metformin), or to FMD in combination with chemotherapy.

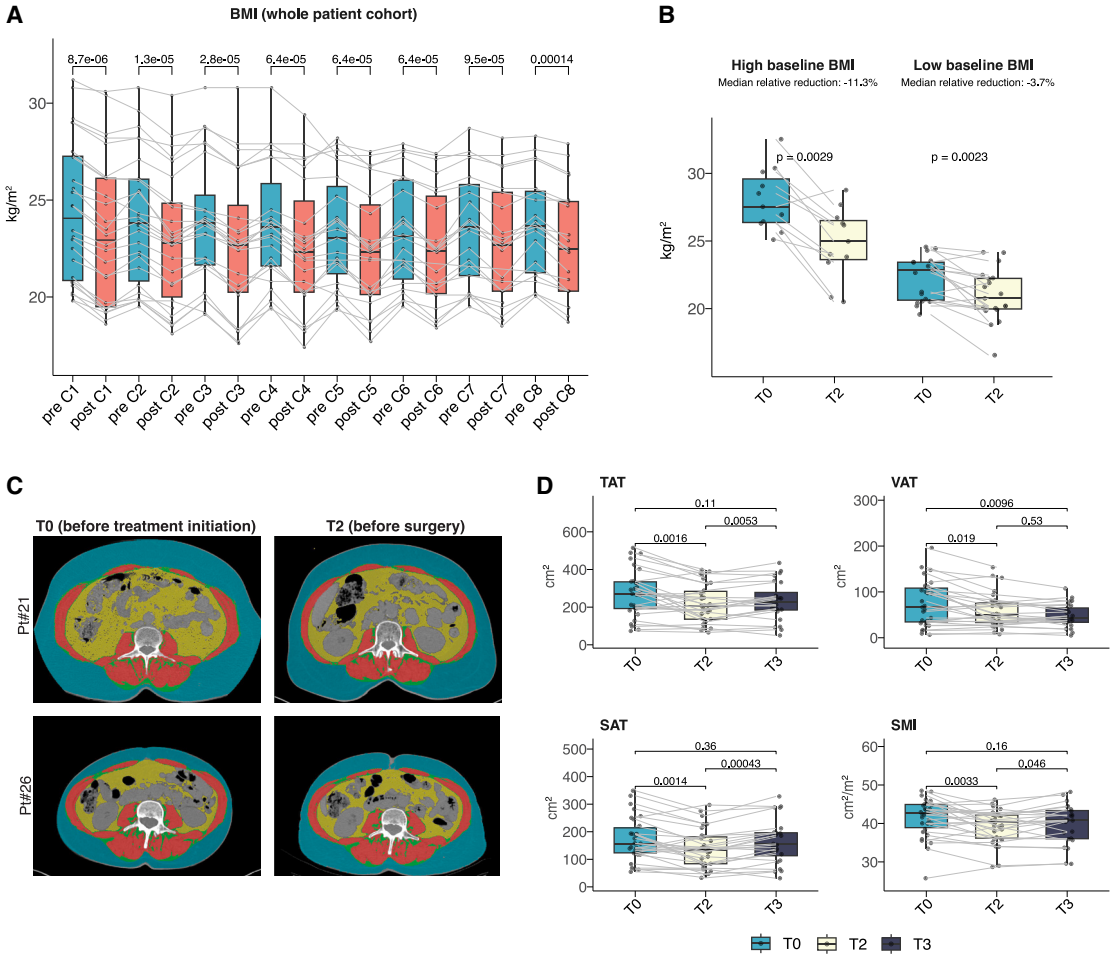

Figure 3. Changes in patient BMI and body composition parameters

(A) Boxplots representing short-term BMI changes during the experimental treatment in $n = 26$ patients. BMI was evaluated before ("pre") and after ("post") each of eight consecutive FMD cycles. p values referring to the paired Wilcoxon test for each of the indicated comparisons are reported.

(B) Boxplots representing long-term BMI changes (i.e., BMI measured before surgery—T2 vs. baseline—T0) during the experimental treatment in overweight/obese patients ("high BMI": ≥ 25 kg/m^2; $n = 11$) or in patients with normal baseline weight ("low BMI": <25 kg/m^2; $n = 19$). Each boxplot indicates the 25th and 75th percentiles of the BMI distribution, while the horizontal line inside the box indicates the median value of the distribution. Dots indicate BMI measurements in individual patients. p values refer to the paired Wilcoxon test.

(C) Representative CT scan images at L3 level performed at baseline (T0) and before surgery (T2) in two representative patients (patient #21, normal weight at diagnosis, and patient #26, obese at diagnosis). VAT is indicated in yellow, SAT in blue, SMA in red.

(D) Boxplots representing body composition parameters measured in matched CT scan images collected at baseline (T0; $n = 30$), before surgery (T2; $n = 30$) and 3–12 months after surgery (T3) ($n = 24$).

BMI, body mass index; CT, computed tomography; SAT, subcutaneous adipose tissue; SMA, skeletal muscle area; SMI, skeletal muscle index; TAT, total adipose tissue; VAT, visceral adipose tissue. SMI is calculated as SMA/height.[2]

In addition, pCR rates in the CTRL cohort were numerically similar in patients with high vs. normal baseline BMI (39.3 vs. 35.4%, respectively; $p = 0.93$) (Figure S4E).

Then, we analyzed computed tomography (CT) scans performed at baseline (T0), at surgery (T2), and at a later time point (T3: on average 12 months during the follow-up after surgery) to measure body composition parameters reflecting adipose tissue and skeletal muscle, and to evaluate their modifications during the experimental treatment (Figure 3C). Total adipose tissue (TAT), visceral adipose tissue (VAT), subcutaneous adipose tissue (SAT), and skeletal muscle index (SMI) measured at baseline showed a strong, positive correlation with baseline BMI (Figures S4F–S4I). All these parameters were reduced during the experimental treatment (Figures 3C and 3D), but their reduction reached statistical significance only in patients who were overweight/obese at baseline (BMI $\geq$ 25 kg/m^2) (Figure S4J). While the reduction of TAT, SAT, and SMI was in part recovered at longer follow-up (T3), the reduction of VAT maintained stable (Figure 3D).

Together, these data indicate that baseline BMI affects the modifications of BMI and body composition parameters during FMD plus chemotherapy and that overweight/obese patients may potentially achieve higher benefit from cyclic FMD in combination with chemotherapy.

Systemic metabolism is reshaped during FMD plus chemotherapy

The FMD caused a significant reduction of blood glucose, insulin, and insulin-like growth factor 1 (IGF-1) concentration, paralleled by an increase of urinary ketone bodies (Figure S5A). These metabolic modifications, which were rapidly reversed upon refeeding and well reproducible across subsequent FMD cycles, recapitulate systemic metabolic modifications that were previously reported in a heterogeneous cohort of 101 cancer patients undergoing the same, cyclic FMD regimen in combination with different standard therapies.[11] Of note, these metabolic changes were comparable in the two treatment arms, thus indicating that metformin does not significantly affect chemotherapy plus FMD-induced modification of systemic metabolic parameters (Figures S5B and S5C). In addition to the expected reduction of blood glucose and growth factor concentration, we also observed a significant and reversible reduction of blood lactate dehydrogenase (LDH) levels (Figures S5A–S5C). Although we cannot exclude that blood LDH reduction during the FMD is the result of reduced LDH release from other organs, such as the liver and the muscle, we believe that it is more likely to be attributable to the FMD, rather than to chemotherapy, for the following reasons: (1) LDH kinetics were characterized by an early and rapidly reversible drop (Figure S5A), i.e., similar to the case of other metabolic parameters, such as blood glucose and growth factors, which are known to be specifically modulated by the FMD in cancer patients[11]; (2) in a cohort of advanced TNBC patients enrolled in an observational study, and undergoing blood collection for biochemical evaluations 2 days before and 3 days after chemotherapy administration (i.e., with the same kinetics adopted in patients undergoing chemotherapy plus FMD in the BREAKFAST trial[11]), chemotherapy did not cause an acute decrease of blood LDH levels, and it even resulted in a trend toward an increase of blood LDH (Figure S5D). Together, these data suggest that blood LDH reduction may reflect FMD-induced inhibition of tumor glycolysis.

Cyclic FMD plus chemotherapy reshapes intratumor metabolism

To investigate the effects of the experimental treatment on intratumor metabolism, we performed global RNA sequencing (RNA-seq) analysis in fresh-frozen tumor biopsy specimens collected at baseline (T0: before treatment initiation) and before the second treatment cycle (T1: ~14–20 days after treatment initiation). To verify the biological reliability of transcriptomic data, in T0 tumor specimens we applied previously published classifications of human TNBC specimens based on tumor transcriptomic profiles. As shown in Figure S6A, the percentages of TNBC subtypes classified according to "intrinsic subtypes classification,"[26] "Lehman's classification,"[27,28] and "metabolic classification"[29] were in line with the proportion of these biological subtypes in previously published studies in human TNBC series.[26,27,29] In addition, deconvolution analyses of transcriptomic data[30] showed that several intratumor immune cell populations were increased early during the study treatment (Figure S6B), thus recapitulating results that we previously reported in patients undergoing one FMD cycle without concomitant systemic therapies.[11] Interestingly, we found a trend toward an increase of several tumor-infiltrating immune cells, such as dendritic cells, T helper (Th) 1 cells, natural killer (NK) cells, NKT cells, CD8+, and CD4+ central and effector memory T cells only in tumor specimens collected from patients achieving pCR (Figure S6C).

Then, we moved to study the effect of the experimental treatment on cancer metabolism, which was evaluated in tumor specimens through the use of transcriptomic data. To investigate whether transcriptomic data reliably reflect intratumor metabolic changes occurring during fasting, we used a mouse model of TNBC that is known to be sensitive to cyclic fasting/FMD, namely orthotopic murine 4T1 cells injected in the mammary fat pad of female BALB/c mice.[2,3] Since the reduction of blood glucose plays a crucial role in mediating the anticancer effects of cyclic fasting/FMD in TNBC models,[2] in this experiment, we investigated whether metabolomic and transcriptomic analyses are similarly able to capture the downmodulation of intratumor glucose metabolism that is induced by fasting. When mammary tumor masses became palpable, mice were randomly assigned to *ad libitum* diet (CTRL), or to 48-h water-only fasting, which was repeated cyclically (every 1 week). As previously reported,[3] cyclic fasting slowed down tumor progression (Figures S7A and S7B) and prolonged animal survival (Figure S7C). In the same experiment, we used an additional number of animals exposed to CTRL or fasting, and which were precociously sacrificed to collect blood samples and tumor masses at the end of the second fasting cycle to perform mass spectrometry-based metabolomic and bulk RNA-seq analysis. We found a significant reduction of glucose concentration in the blood (Figure S7D) and in the tumor (Figure S7E) in fasted animals, and this was paralleled by a depletion of glucose metabolism-related pathways according to Kyoto Encyclopedia of Genes and Genomes (KEGG) (Figure S7F) and Hallmark (Figure S7G) classifications by gene set enrichment analysis (GSEA) of transcriptomic data.

Having established that bulk RNA-seq data reliably reflect changes in intratumor glucose metabolism during fasting in TNBC models that are sensitive to nutrient starvation, we moved to investigate changes in the expression of metabolic pathways and individual metabolic genes in tumor specimens from BREAKFAST trial patients. GSEA according to KEGG (Figure 4A; Figure S8A) or Hallmark (Figure 4A; Figure S8B) collections revealed an early, negative enrichment of pathways related to glucose metabolism, glycolysis, tricarboxylic acid (TCA) cycle, and OXPHOS. Biological pathways reflecting mTORC1 activity, protein synthesis, and ribosome biogenesis were downregulated as well (Figures S8A and S8B). To confirm and expand these findings, we performed single-sample-level gene set variation analysis (GSVA) evaluating a manually curated selection of 231 metabolic pathways extracted from the Reactome gene set collection. This analysis revealed a downregulation of pathways reflecting glucose, pyruvate, TCA cycle, and OXPHOS metabolism (Figure 4B). Of note, glucose-metabolism-related pathways were only downregulated in "glycolytic" (MPS2) tumors according to metabolic TNBC classification,[29] whereas mitochondrial OXPHOS and electron transport chain (ETC) pathways were only downregulated in MPS1/3 (lipogenic or mixed) tumors (Figure S8C).

The observed metabolic modulations could be attributable to chemotherapy, to the FMD, or to their combination. Since the BREAKFAST trial lacked a CTRL arm, we analyzed 12 matched

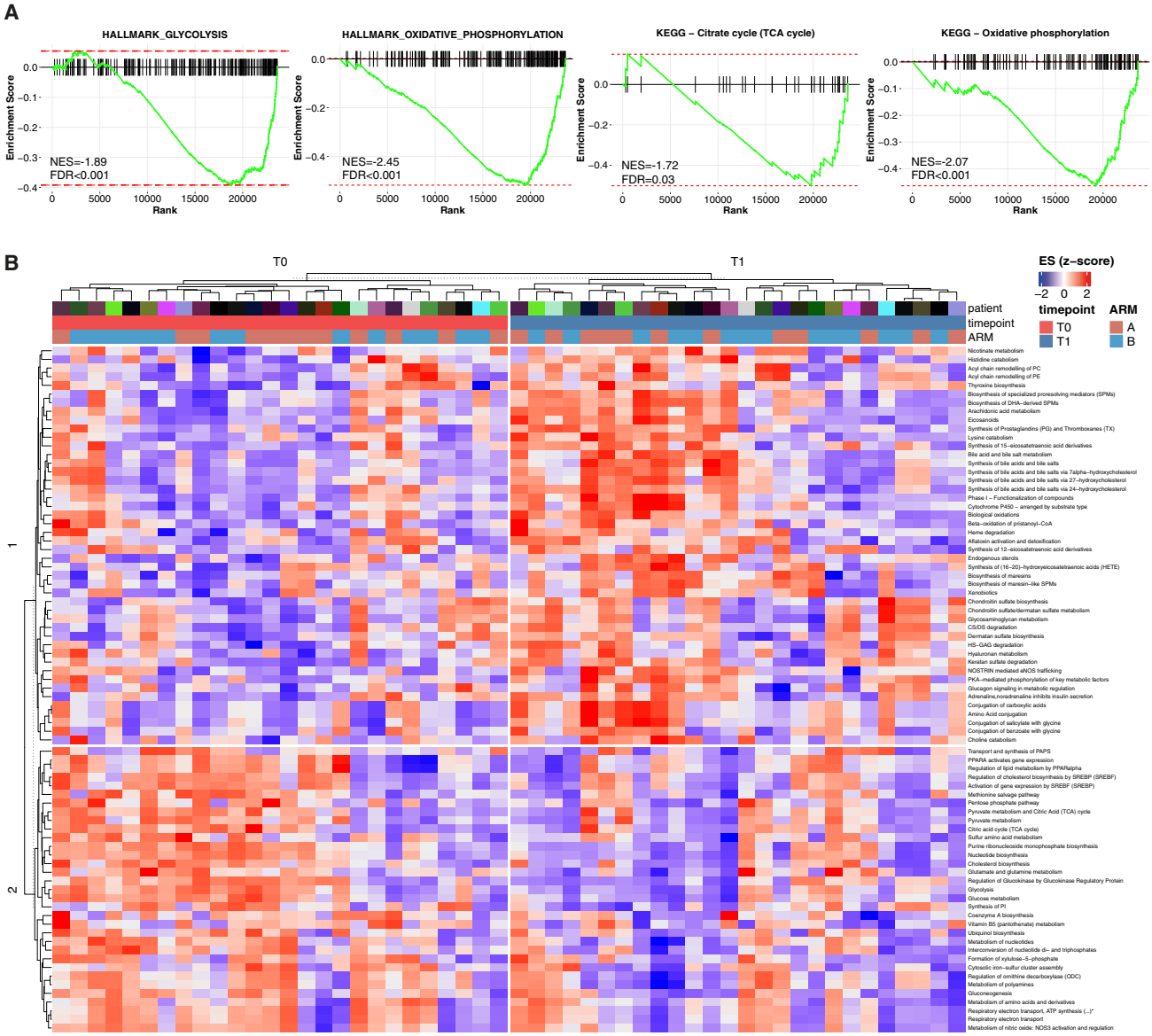

Figure 4. Early modulation of intratumor metabolic pathways

(A) Enrichment plot of selected metabolic KEGG and Hallmark pathways that are significantly (p adjusted < 0.05) downmodulated in T1 vs. T0 tumor biopsy specimens by GSEA, which was performed in 29 and 26 tumor specimens at T0 and T1, respectively.

(B) Heatmap representing metabolic pathways of the Reactome collection whose GSVA ESs were significantly modulated (paired Wilcoxon test $p < 0.05$ and Benjamini-Hochberg [B-H] false discovery rate [FDR] < 0.1) in T1 vs. T0 samples ($n = 26$ matched samples).

ES, enrichment score; GSEA, gene set enrichment analysis; GSVA, gene set variation analysis.

tumor biopsy specimens (obtained at baseline or after 3 days after the first chemotherapy administration) from an external CTRL cohort of TNBC patients treated with anthracycline-based chemotherapy in the context of the I-SPY1 trial,[31] and whose tumor specimens were subjected to bulk transcriptomic analysis. While pathways related to OXPHOS and ETC were negatively enriched in tumor biopsies collected after the administration of the first treatment cycle, glycolysis, pyruvate, and TCA cycle metabolism pathways were not. Together with results of transcriptomic analyses conducted in BREAKFAST trial tumor specimens, these findings suggest that early downregulation of intratumor OXPHOS may predict TNBC response to chemotherapy plus/minus FMD, while the downregulation of glucose/pyruvate metabolism could specifically reflect glycolysis inhibition in tumors exposed to FMD plus chemotherapy (Figure S8D).

Inhibition of intratumor glucose metabolism predicts pCR

In murine TNBC models, FMD-induced reduction of blood glucose concentration and intratumor glycolysis was found to be a crucial determinant of the antitumor effects of nutrient starvation.[2] Here, we tested whether changes in systemic and

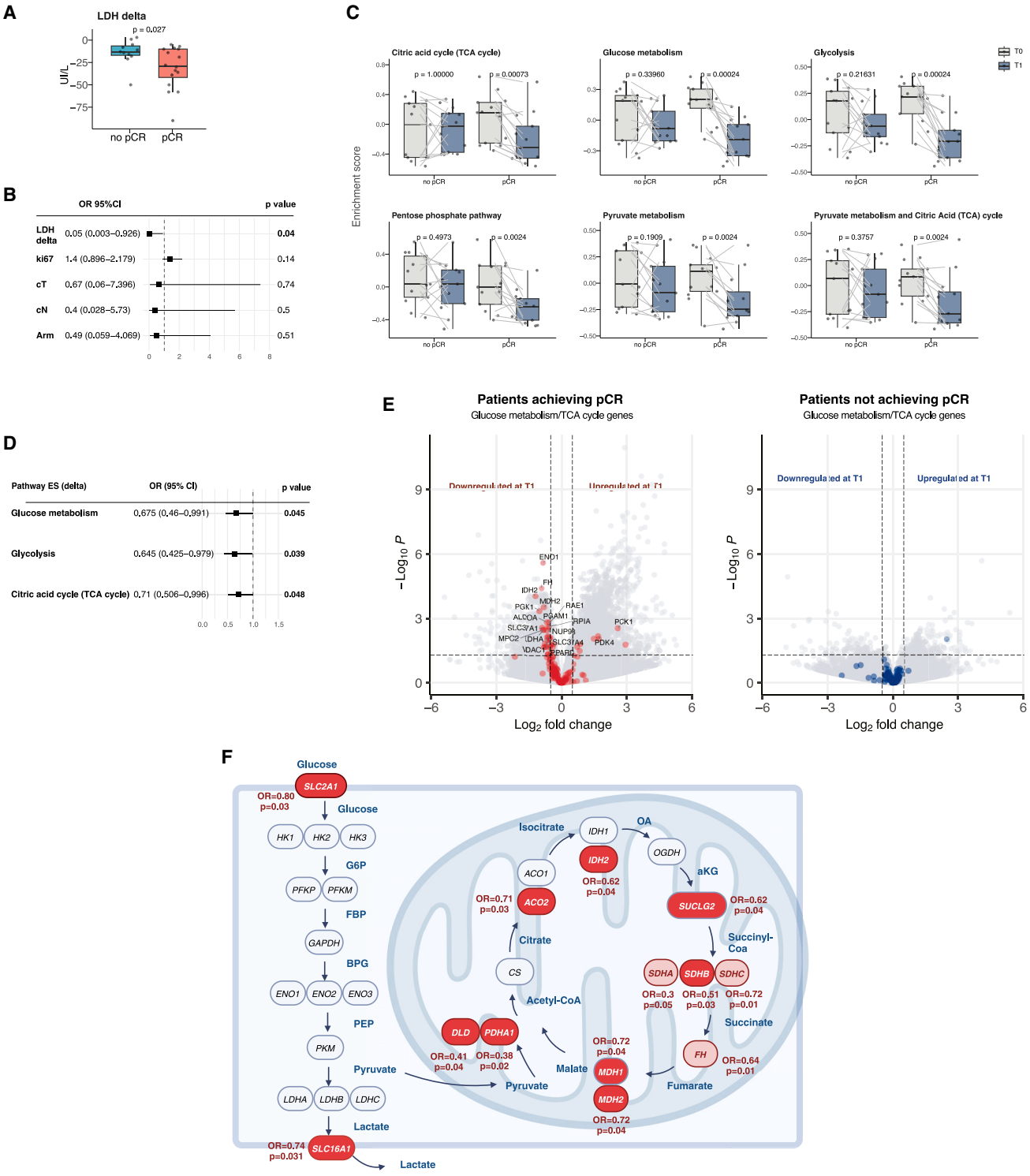

Figure 5. Association between early downregulation of systemic/intratumor glucose metabolism and pCR probability

(A) Boxplots representing absolute deltas of blood LDH concentration (post-FMD minus pre-FMD blood LDH levels) according to pCR status (n = 27 patients). p values refer to unpaired Wilcoxon test.

(B) Multivariable logistic regression model for pCR including blood LDH delta, Ki-67 expression, tumor size (cT), nodal status (cN), and treatment arm as adjustment covariates.

(C) Boxplots representing GSVA ESs of glucose metabolism pathways before treatment initiation (T0) and after one treatment cycle (T1) from n = 26 matched samples and according to pCR status. p values refer to paired Wilcoxon test.

(legend continued on next page)

intratumor metabolism are associated with pCR outcomes. We found a more pronounced, early reduction of blood LDH levels after the first FMD cycle in patients achieving pCR as compared with patients not achieving pCR (Figure 5A). In addition, higher LDH reduction was independently associated with higher pCR rates after adjustment for clinically relevant covariates, such as T and N stage, Ki-67, and treatment arm (Figure 5B). At the tumor level, early downmodulation of pathways reflecting glucose, pyruvate, and TCA cycle metabolism was only observed in patients undergoing pCR, and it was associated with higher pCR probability (Figures 5C and 5D). Consistent with the lack of clinical benefit (Figure 2) and additional systemic metabolic effects (Figures S5B and S5C) resulting from the addition of metformin to chemotherapy plus FMD, metformin use did not result in additional metabolic changes (Figure S9A), and several intratumor pathways related to glycolysis, glucose, and pyruvate metabolism were not differentially enriched after the first treatment cycle in patients treated with or without metformin (Figure S9B). Several individual genes belonging to glucose, pyruvate, and TCA cycle metabolism pathways were modulated after the first treatment cycle only in patients achieving pCR, with the vast majority of them being downregulated (Figures 5D, 5E, and S9C–S9E). Of note, a higher reduction in the expression of glucose transporters, glycolysis, and TCA cycle genes was independently associated with higher pCR probability at multivariable analysis (Figure 5F).

While the majority of metabolic pathways related to glucose, pyruvate, and TCA cycle metabolism underwent early downregulation in patients achieving pCR regardless of patient BMI at baseline (high vs. low) (Figure S10A), the depletion of these metabolic pathways only reached statistical significance in patients with high baseline TAT/VAT and achieving pCR (Figures S10B and S10C). Regarding SAT and SMI, intratumor metabolic pathways were downregulated early in patients undergoing pCR regardless of baseline values of the same parameters (Figures S10D and S10E).

Together, our findings indicate that tumors achieving pCR undergo early downmodulation of metabolic pathways related to glucose/pyruvate metabolism, and this may be especially true in patients with higher baseline total and visceral adiposity.

FMD downmodulates glycolysis in TNBC cells and in highly glycolytic intratumor cells

To investigate the modulation of glucose-related metabolic pathways in cancer cells and in cellular populations of the tumor microenvironment (TME), we resorted to single-cell RNA-seq (scRNA-seq) analysis, which was performed in fresh tumor samples collected at baseline (T0; $n = 13$) and after one treatment cycle (T1; $n = 11$). Overall, we obtained transcriptomic profiles from 177,981 viable cells, which were subsequently annotated and classified into major cell types (epithelial cells, fibroblasts, T cells, B cells, plasma cells, myeloid cells, endothelial cells, pericytes, and adipose cells) (Figure 6A). Among 26,013 epithelial cells, we identified 18,055 cancer cells (representing 10.1% of all sequenced cells) based on their copy-number alterations (CNAs) profiles.[32] Baseline GSVA scores related to glucose/pyruvate metabolism pathways revealed that intratumor myeloid cells, myoepithelial cells, cancer cells, and pericytes are the most glycolytic cellular subtypes, in line with published data (Figure 6B).[33–35] Notably, cancer cells, myeloid cells, and pericytes underwent significant depletion of pathways related to glucose metabolism (“glycolysis,” “glucose metabolism,” “pentose phosphate pathway,” “citric acid cycle (TCA cycle),” “pyruvate metabolism and citric acid (TCA) cycle”; Reactome pathway database) in tumors undergoing pCR, whereas the same pathways were enriched in the same cellular subsets in tumors not undergoing pCR ($p$adj < 0.05; average logFC > 0.25 or < –0.25) (Figures 6C and 6D). On the other hand, cells with lower baseline glycolytic metabolism, such as non-neoplastic epithelial cells, T and B lymphocytes, did not undergo a significant modulation (up or down) of these metabolic pathways during the study treatment (Data S1).

DISCUSSION

We showed that cyclic FMD, with or without metformin, is safe and results in excellent pCR rates, EFS, and OS when combined with preoperative anthracycline-cyclophosphamide-taxane chemotherapy in patients with early-stage TNBC. Early downregulation of systemic and intratumor glucose/pyruvate metabolism is associated with higher pCR rates regardless of metformin use. In patients undergoing pCR, cancer cells and more glycolytic tumor-infiltrating cells experience the strongest downregulation of metabolic pathways related to glucose metabolism and pyruvate oxidation during chemotherapy plus cyclic FMD.

Severe FMD-related AEs were rare in BREAKFAST trial patients, thus confirming and expanding previous safety findings from a much more heterogeneous cohort of cancer patients undergoing the same, severely calorie-restricted 5-day FMD regimen in combination with standard antineoplastic treatments.[11] In a recently published preclinical work, intermittent fasting (every-other 24 h) followed by refeeding resulted in increased cardiac toxicities in mice receiving anthracycline-based chemotherapy.[36] In these experiments, heart toxicity was caused by fasting-induced increase of nuclear transcription factor EB (TFEB), which resulted in an impaired cardiac function and in an increase of animal mortality.[36] In the BREAKFAST trial, at the end of four triweekly cycles of doxorubicin plus

(D) Univariate logistic regression model evaluating the association between early downregulation of selected Reactome metabolic pathways (measured as the delta of GSVA ES in T1 vs. T0 tumor samples; the OR refers to each 0.1 ES increase) and pCR probability.
(E) Volcano plots displaying differentially expressed genes comparing T1 vs. T0 gene-level RNA-seq data using negative binomial distribution (Deseq2 algorithm). Glucose metabolism-related genes (i.e., those included in the Reactome metabolic pathways) in (C) are colored in red (left, samples from patients achieving pCR), or in blue (right, samples from patients not achieving pCR); genes differentially expressed with p value < 0.05 and FDR < 0.1 are labeled.
(F) Chart highlighting genes involved in glucose transport, glycolysis, pyruvate metabolism, and TCA cycle, whose early downregulation during the experimental treatment was associated with higher pCR probability by univariate (light red) or multivariable (dark red) regression model adjusting for tumor size, nodal status, treatment arm and Ki67 expression. ORs and p values are reported. Each boxplot (A and C) indicates the 25th and 75th percentiles of the distribution of the variable, while the horizontal line inside the box indicates the median values. Dots indicate individual variable values.
ES, enrichment score; GSVA, gene set variation analysis; pCR, pathologic complete response; OR, odds ratio.

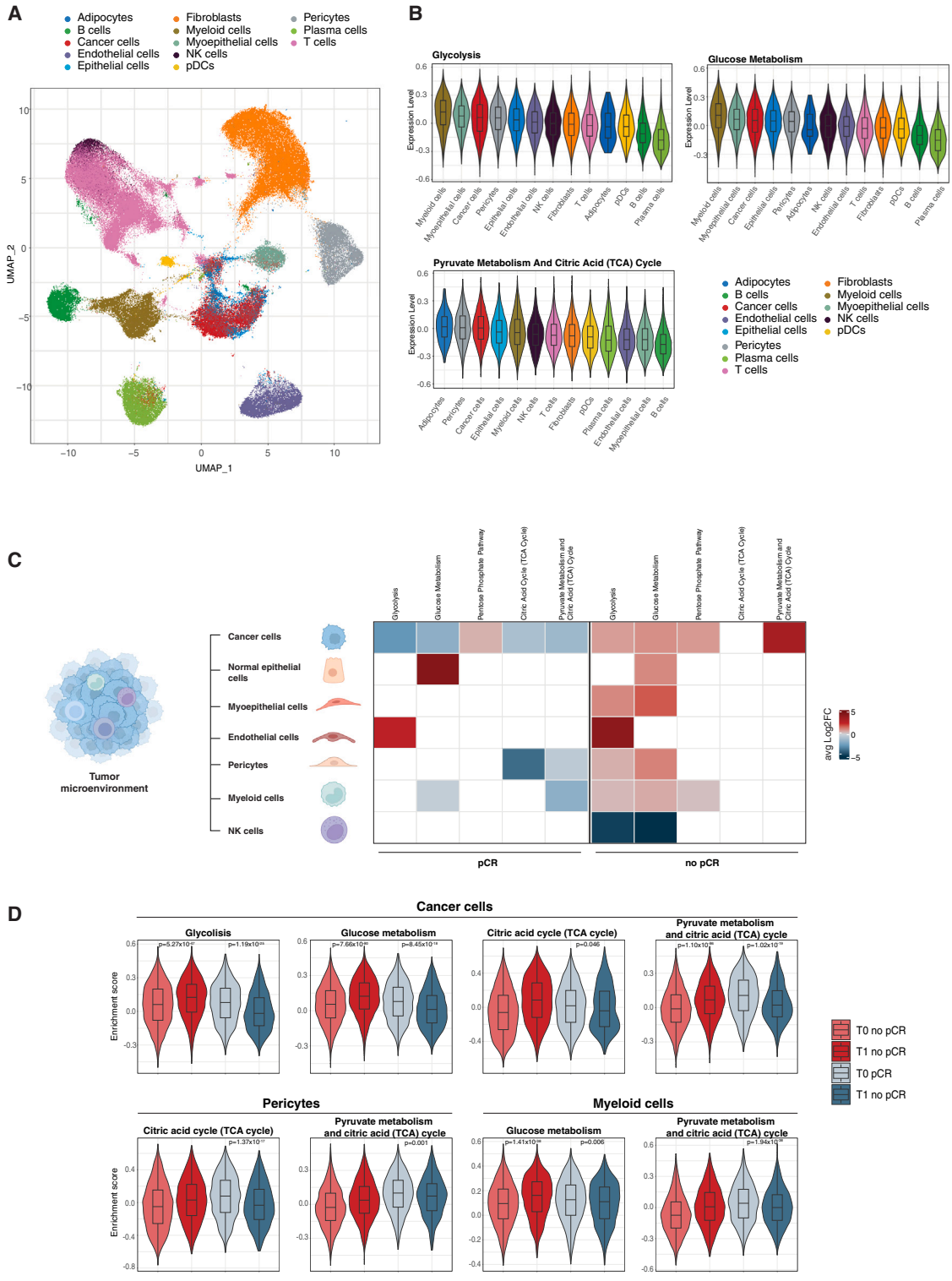

Figure 6. Modulation of intratumor glucose metabolism in different tumor-infiltrating cells

(A) Uniform manifold approximation and projection (UMAP) plot of individual intratumor cells from $n = 25$ tumor specimens (T0: $n = 14$, T1: $n = 11$) classified into the indicated cell subtypes.

(B) GSVA ESs of Reactome pathways related to glucose metabolism, glycolysis and TCA cycle activity, as measured in baseline tumor specimens (T0) in individual cells of the indicated cellular subtypes. The distribution of ESs according to each cell subtype is represented with violin plots and boxplots, where upper

(legend continued on next page)

cyclophosphamide in combination with 5-day FMD, we did not observe a significant reduction in patient cardiac function. These data are in line with results of preclinical studies showing that the combination of anthracyclines and fasting/FMD cycles of longer duration (48–96 h) does not increase anthracycline-induced cardiac toxicity in mice.[1,3] To explain these data, we hypothesize that a rebound in specific blood metabolites occurring during the refeeding intervals between subsequent, short-term (24 h) fasting cycles may be toxic for cardiomyocytes exposed to concomitant anthracycline treatment, whereas fasting/FMD regimens of longer duration, such as 48-h fasting in mice, or 5-day FMD in patients, could even protect cardiomyocytes from anthracycline-induced toxicity.

The median number of FMD cycles that were successfully completed by patients enrolled in the BREAKFAST trial was significantly higher than that reported in the NCT03340935 study (median: 8 vs. 4 cycles, respectively) or in the phase 2 trial "DIRECT" trial (median: 2 FMD cycles), which was precociously interrupted because of poor patient compliance with the experimental FMD regimen.[37,38] The continuous progress achieved in the management of patients undergoing cyclic FMD in recently conducted clinical trials, which at least in part depends on an increasing ability and expertise by physicians and nutritionists involved in these studies in effectively preventing or timely managing FMD-related AEs, is crucial to expand the clinical investigation of this experimental nutritional intervention in patients with different tumor types and treated with different anticancer therapies.

Although the BREAKFAST trial lacked a CTRL arm and enrolled a small number of patients, the observed pCR rate outperformed the results of previously published studies employing similar or even more effective (e.g., dose-dense) preoperative anthracycline-cyclophosphamide-taxane chemotherapy regimens in patients with early-stage TNBC,[17–22,25] including an independent retrospective TNBC cohort of patients treated at our institution.[24] In terms of long-term clinical outcomes, the observed EFS and OS are especially promising, and they compare well with long-term clinical outcomes reported in recent trials investigating highly effective, preoperative chemo-immunotherapy regimens, which have recently become the new standard-of-care therapy in early-stage TNBC patients.[15,16]

In this study, we observed early reduction of blood LDH concentration, paralleled by a downregulation of pathways reflecting intratumor glucose metabolism, only in patients undergoing pCR. scRNA-seq analysis revealed that the most glycolytic intratumor cells, namely cancer cells, myeloid cells and pericytes, experience the strongest, early downregulation of glucose/pyruvate metabolism pathways in tumors undergoing pCR at the end of the study treatment. These findings are in line with preclinical literature indicating that (1) highly glycolytic malignancies, such as TNBCs, are exquisitely sensitive to glucose deprivation and fasting conditions,[2,3] and (2) peripheral blood monocytes and intratumor myeloid cells are exquisitely sensitive to glucose deprivation and glycolysis inhibition.[11,39,40] In a recent clinical work, we showed that cyclic FMD reduces peripheral blood myeloid-derived suppressor cells.[11] However, the impact of the FMD on the metabolic properties of tumor-infiltrating myeloid cells in cancer patients was not explored. Consistent with preclinical data indicating that monocytes and myeloid cells are exquisitely dependent on glucose metabolism,[39,40] here, we provided first evidence that myeloid cells from tumors responding to chemotherapy plus FMD undergo a reduction in their glycolytic activity. In this study, we also observed a global inhibition of glucose metabolism in pericytes from tumors responding to the treatment. Intratumor pericytes play a crucial role in shaping the TME and in modulating drug delivery to cancer cells.[41] In particular, recent data indicate that glycolysis inhibition in pericytes enhances blood vessel function, thus potentially boosting chemotherapy effectiveness.[33,35] Together with published data, our findings suggest that the FMD may affect the functional properties of tumor vasculature, with potentially relevant effects in terms of chemotherapy delivery to tumor cells and cytotoxic activity.

The use of fasting/FMD regimens in cancer treatment has been historically criticized because of the potential risk of causing or precipitating sarcopenia or cachexia.[42] Here, we showed that triweekly cycles of a severely calorie-restricted, 5-day FMD regimen in combination with chemotherapy result in a reduction of patient BMI, as well as of global and visceral adiposity and skeletal muscle. Of note, FMD-induced loss of skeletal muscle was mostly recovered at longer follow-up, while the reduction of visceral fat was maintained. In a previously published clinical trial (NCT03595540), cyclic FMD did not significantly modify body composition parameters.[8] However, the FMD regimen used in the NCT03595540 trial contained approximately the double number of daily calories as compared with the FMD regimen investigated in the BREAKFAST trial. Findings of the BREAKFAST trial are clinically reassuring, because they indicate that a severely calorie-restricted, 5-day FMD regimen in combination with chemotherapy does not result in progressive, long-term loss of skeletal muscle in patients early-stage TNBC.

Patients who were overweight/obese at baseline had higher adiposity and muscle mass, which is consistent with previously published studies.[43] In addition, we observed numerically higher pCR rates in overweight/obese patients, although this difference did not reach statistical significance, probably because of the low number of patients included in this analysis. Although very preliminary, this observation is interesting and, in our opinion, it

and lower boxplot limits indicate the 25th and 75th percentiles of the variable distribution, while the horizontal line inside the box indicates the median values of the distribution.

(C) Heatmap displaying selected glucose metabolism-related pathways that are significantly (i.e., adjusted p value < 0.05 according to the FindMarkers R function algorithm and $|\log_2 FC| > 0.25$) upregulated or downregulated in specific cellular types in T1 vs. T0 samples from patients achieving or not achieving pCR. Average $\log_2 FC$ of GSVA ES (T1 vs. T0) for each pathway in each cell population is represented.

(D) Violin plots and boxplots representing the distribution of GSVA ESs of selected glucose metabolism-related pathways in cancer cells, myeloid cells, and normal epithelial cells, according to time point (T1 vs. T0) and pCR status. The adjusted p value is indicated when significant according to the FindMarkers R function algorithm. Upper and lower boxplot limits indicate the 25th and 75th percentiles of the distribution of the variable, while the horizontal line inside the box indicates the median values. p values are obtained by Wilcoxon rank-sum test.

ES, enrichment score; GSVA, gene set variation analysis; pCR, pathologic complete response.

deserves further investigation in future clinical trials enrolling higher numbers of patients. Indeed, if confirmed in future and properly powered trials also including a CTRL arm, a differential benefit of FMD-based treatments in normal weight vs. overweight/obese patients may reveal a novel and clinically usable biomarker capable of predicting clinical benefit from calorie-restricted regimens. This biomarker could be used for the selection of patients more likely to benefit from the addition of cyclic FMD to standard pharmacologic treatments.

In preclinical experiments, the OXPHOS complex I inhibitor metformin showed highly synergistic antitumor effects when combined with *in vitro* glucose starvation or *in vivo* cyclic fasting.[14,44] In addition, retrospective and prospective studies showed promising antitumor activity of metformin in some clinical cohorts, such as in patients with well differentiated neuroendocrine tumors (NETs).[45,46] In the BREAKFAST trial, metformin did not significantly affect tumor pCR rate, nor treatment-induced modulation of systemic or intratumor metabolism. These results are consistent with findings of several prospective studies conducted in recent years, which globally showed that metformin, as used at dosages that are commonly used for type 2 diabetes mellitus (T2DM) therapy, does not exert meaningful antitumor activity in patients with different tumor types,[47–49] including breast cancer.[50] While we cannot exclude that the low number of patients enrolled in the BREAKFAST trial may have reduced the power to detect differences, in terms of pCR or EFS, between patients receiving or not receiving metformin, our findings indicate that metformin, when used at well-tolerated dosages commonly employed for the treatment of T2DM, does not produce clearly synergistic biological or antitumor effects in combination with cyclic FMD. Different hypotheses may explain the lack of biological or antitumor activity of metformin: (1) blood metformin concentrations that are achieved through the use of well-tolerated oral metformin dosages may not be sufficiently high to produce meaningful anticancer effects in patients[14]; (2) the FMD scheme used in the BREAKFAST trial (5 consecutive days repeated every 3 weeks) may not be long enough to cause synergistic antitumor effects when combined with metformin, which in preclinical experiments was effective only when administered during every-other-day intermittent fasting[14,51]; (3) while TNBC is exquisitely sensitive to cyclic fasting/FMD in combination with chemotherapy, metformin may not synergize with fasting/FMD in this tumor type,[2] as instead observed in preclinical colorectal carcinoma or melanoma models.[14] Together, results of the BREAKFAST trial, as well as of published preclinical experiments, do not support further clinical investigation of metformin in combination with cyclic FMD in TNBC patients.

In conclusion, BREAKFAST is the first phase 2 clinical trial to provide proof-of-concept evidence that cyclic FMD plus chemotherapy (1) is safe and active when combined with preoperative anthracycline-taxane chemotherapy in early-stage TNBC patients, (2) results in significant reduction of patient BMI, adipose tissue and skeletal muscle especially in patients who are overweight or obese at baseline; (3) causes early downregulation of metabolic pathways related to glucose/pyruvate metabolism and TCA cycle in individual cancer cells and in other highly glycolytic tumor-infiltrating cells only in patients achieving pCR. Based on these findings, as well as on solid preclinical evidence showing that cyclic FMD has cooperative antitumor effects when combined with chemotherapy or immunotherapy in TNBC models,[1–3,9] we recently initiated BREAKFAST-2 (NCT05763992), a multicentric, randomized phase 2 clinical trial, to investigate whether adding cyclic, 5-day FMD to standard preoperative chemoimmunotherapy increases tumor pCR rates in patients with stage II and III TNBC, and to validate early downmodulation of intratumor glucose metabolism as a biomarker predictive of clinical benefit from FMD-based combination treatments.

Limitations of the study

Limitations of this study are (1) the lack of a CTRL arm of patients treated with chemotherapy alone; (2) the small number of patients enrolled; (3) its precocious interruption due to changes in the standard-of-care therapy of early-stage TNBC; (4) the use of a backbone neoadjuvant chemotherapy regimen that has been now replaced by novel and more effective chemotherapy regimens that also include carboplatin and the anti-PD-L1 immune checkpoint pembrolizumab.

RESOURCE AVAILABILITY

Lead contact

Further information and requests for resources and reagents should be directed to and will be fulfilled by the lead contact, Claudio Vernieri (claudio.vernieri@istitutotumori.mi.it; claudio.vernieri@ifom.eu).

Materials availability

This study did not generate new unique reagents.

Data and code availability

BREAKFAST trial bulk and single-cell RNA-seq data (FASTQ files) have been deposited to the European Genome-phenome Archive (EGA) database. Accession numbers are listed in the key resources table. Mouse bulk RNA-seq data (FASTQ files) have been deposited to ArrayExpress. Accession numbers are listed in the key resources table. Other source data are provided in "Data S1, source data."

This paper also analyzed existing, publicly available data. The accession numbers for these datasets are listed in the key resources table.

This paper does not report original codes.

ACKNOWLEDGMENTS

We thank all the patients that took part in the BREAKFAST trial and their families. We thank Simone Minardi, Marco Pierotti, and Claudia Valli and the Genomic Unit of Cogentech for performing bulk RNA sequencing; we thank Raoul Bonnal, Riccardo Rossi, and Cristiano Petrini (Research Computing and Data Science facility at IFOM) for the help in uploading raw data in appropriate public repositories. We also thank Angela Bachi and Laura Tronci from the Proteomic and Metabolomic Unit of Cogentech for performing plasma and intratumor quantification of glucose concentration in murine tumor specimens. This work was supported by funds of the Italian Ministry of Health (Ricerca Corrente), the Scientific Directorate of Fondazione IRCCS Istituto Nazionale dei Tumori (Milan, Italy), and the "Associazione Italiana per la Ricerca sul Cancro" (AIRC; MFAG-2019 no. 22977: principal investigator: C.V.). F.L., G. Salvadori, and M.R. are supported by an AIRC Italy post-doc fellowship. We also thank the European Research Council (ERC), the Giuliani Foundation—Fondazione Gianmaria e Sabrina Giuliani—and Celeste Ungaro and Maria Annunziata Caforio for supporting our research on cancer metabolism.

AUTHOR CONTRIBUTIONS

Conceptualization: C.V., S.M., M.F., G.P., and F.d.B.; data curation: F.L., C.S., L.Z., L.P., R.L., G. Fucà, and G. Fotia; formal analysis: F.L., T.T., A.V., L.D., F.I., M.R., and F.N.; funding acquisition: C.V., M.F., G.P., G.A., and

F.d.B.; investigation: F.L., A.V., C.V., and T.T.; methodology: C.V., F.L., A.V., and L.M.; project administration: C.V., G.P. and F.d.B.; resources: C.D., S.F., G. Scaperrotta, G.C., G.V.B, C.F., G. M., I.M., D.M., V.L., M.C.D.S., L.L., G.T., A. Belfiore, S.B., A. Bertolotti, A.F., A.M., E.S., A.A., P.C., L.S., and G. Salvadori; software: F.L., T.T., A.V., L.D., F.I., F.N., and L.A.; supervision: C.V.; validation: F.L. and A.V; visualization: F.L. and T.T.; writing – original draft: F.L. and C.V.; and writing – review & editing: all authors.

DECLARATION OF INTERESTS

The authors declare the following competing interests: G.V.B., speaker/advisory board: Novartis, Eli Lilly, Daichi/Astrazeneca, Roche, MSD, and Seagen; G.P., consulting fees: Roche, Bayer, and Astra Zeneca; C.V., consulting fees/advisory board: Novartis, Pfizer, Eli Lilly, Daiichi Sankyo, and Menarini Stemline; C.V., honoraria as speaker: Novartis, Eli Lilly, Istituto Gentili, Accademia Nazionale di Medicina, MSD, Research grant: Roche; F.d.B., consulting fees/advisory board: Roche, EMD Serono, NMS Nerviano Medical Science, Sanofi, MSD, Novartis, Incyte, BMS, Menarini, Astra Zeneca, Pierre Fabre, Mattioli 1885, MCCann Health, Taiho; F.d.B., IQVIA Speaker Bureau: BMS, Healthcare Research & Pharmacoepidemiology, Merck Group, MSD, Pfizer, Servier, Sanofi, Roche, AMGEN, Incyte, Dephaforum, Seagen, Nadirex, BMS, Ambrosetti, and Itanet; and F.d.B., research grant/funding: Novartis, F.Hoffmann-LaRoche Ltd, BMS, Ignyta Inc., Merck Sharp & Dohme Spa, Kymab, Pfizer, Tesaro, MSD, MedImmune LCC, Exelixis Inc., LOXO Oncology Inc., DAICHI SANKIO Dev. Ltd, Basilea Pharmaceutica International AG, Janssen-Cilag International NV, and Merck KGAA. C.V. and F.d.B. are co-inventors of the FMD regimen used in this study. The Italian patent (no. 102019000009954) has been released and was first deposited on June 24th, 2019, with an extension granted under PCT WO 2020/261131 on June 24th, 2020. The European patent (no. 207403399), Canadian patent (no. 2144217), and USA patent are pending.

STAR★METHODS

Detailed methods are provided in the online version of this paper and include the following:

- KEY RESOURCES TABLE
- EXPERIMENTAL MODEL AND STUDY PARTICIPANT DETAILS
  - Study design and patients
  - INT 79/17 trial
  - INT 92/20 study
  - Public transcriptomic data from the I-SPY-1 trial
  - Mouse models
  - Animal diets
- METHOD DETAILS
  - Study endpoints
  - FMD management and analysis of patient compliance
  - Sample size calculation
- QUANTIFICATION AND STATISTICAL ANALYSIS
  - Statistical analysis
  - Biological evaluations in blood samples
  - BMI and body composition analysis
  - Bulk RNA sequencing analysis (BREAKFAST trial)
  - scRNA sequencing analysis (BREAKFAST trial)
  - Bulk RNA sequencing analysis (murine 4T1 tumor specimens)
  - Metabolomics analysis in murine plasma and tumor tissue
- ADDITIONAL RESOURCES

SUPPLEMENTAL INFORMATION

Supplemental information can be found online at https://doi.org/10.1016/j.cmet.2024.11.004.

Received: July 24, 2024
Revised: September 4, 2024
Accepted: November 8, 2024
Published: December 17, 2024

REFERENCES

1. Di Biase, S., Lee, C., Brandhorst, S., Manes, B., Buono, R., Cheng, C.W., Cacciottolo, M., Martin-Montalvo, A., de Cabo, R., Wei, M., et al. (2016). Fasting-Mimicking Diet Reduces HO-1 to Promote T Cell-Mediated Tumor Cytotoxicity. Cancer Cell *30*, 136–146. https://doi.org/10.1016/j.ccell.2016.06.005.
2. Salvadori, G., Zanardi, F., Iannelli, F., Lobefaro, R., Vernieri, C., and Longo, V.D. (2021). Fasting-mimicking diet blocks triple-negative breast cancer and cancer stem cell escape. Cell Metab. *33*, 2247–2259.e6. https://doi.org/10.1016/j.cmet.2021.10.008.
3. Lee, C., Raffaghello, L., Brandhorst, S., Safdie, F.M., Bianchi, G., Martin-Montalvo, A., Pistoia, V., Wei, M., Hwang, S., Merlino, A., et al. (2012). Fasting cycles retard growth of tumors and sensitize a range of cancer cell types to chemotherapy. Sci. Transl. Med. *4*, 124ra27. https://doi.org/10.1126/scitranslmed.3003293.
4. Di Tano, M., Raucci, F., Vernieri, C., Caffa, I., Buono, R., Fanti, M., Brandhorst, S., Curigliano, G., Nencioni, A., de Braud, F., et al. (2020). Synergistic effect of fasting-mimicking diet and vitamin C against KRAS mutated cancers. Nat. Commun. *11*, 2332. https://doi.org/10.1038/s41467-020-16243-3.
5. Ajona, D., Ortiz-Espinosa, S., Lozano, T., Exposito, F., Calvo, A., Valencia, K., Redrado, M., Remírez, A., Lecanda, F., Alignani, D., et al. (2020). Short-term starvation reduces IGF-1 levels to sensitize lung tumors to PD-1 immune checkpoint blockade. Nat. Cancer *1*, 75–85. https://doi.org/10.1038/s43018-019-0007-9.
6. Brandhorst, S., Choi, I.Y., Wei, M., Cheng, C.W., Sedrakyan, S., Navarrete, G., Dubeau, L., Yap, L.P., Park, R., Vinciguerra, M., et al. (2015). A Periodic Diet that Mimics Fasting Promotes Multi-System Regeneration, Enhanced Cognitive Performance, and Healthspan. Cell Metab. *22*, 86–99. https://doi.org/10.1016/j.cmet.2015.05.012.
7. Brandhorst, S., Wei, M., Hwang, S., Morgan, T.E., and Longo, V.D. (2013). Short-term calorie and protein restriction provide partial protection from chemotoxicity but do not delay glioma progression. Exp. Gerontol. *48*, 1120–1128. https://doi.org/10.1016/j.exger.2013.02.016.
8. Caffa, I., Spagnolo, V., Vernieri, C., Valdemarin, F., Becherini, P., Wei, M., Brandhorst, S., Zucal, C., Driehuis, E., Ferrando, L., et al. (2020). Fasting-mimicking diet and hormone therapy induce breast cancer regression. Nature *583*, 620–624. https://doi.org/10.1038/s41586-020-2502-7.
9. Cortellino, S., Raveane, A., Chiodoni, C., Delfanti, G., Pisati, F., Spagnolo, V., Visco, E., Fragale, G., Ferrante, F., Magni, S., et al. (2022). Fasting renders immunotherapy effective against low-immunogenic breast cancer while reducing side effects. Cell Rep. *40*, 111256. https://doi.org/10.1016/j.celrep.2022.111256.
10. Vernieri, C., Ligorio, F., Tripathy, D., and Longo, V.D. (2024). Cyclic fasting-mimicking diet in cancer treatment: Preclinical and clinical evidence. Cell Metab. *36*, 1644–1667. https://doi.org/10.1016/j.cmet.2024.06.014.
11. Vernieri, C., Fucà, G., Ligorio, F., Huber, V., Vingiani, A., Iannelli, F., Raimondi, A., Rinchai, D., Frigè, G., Belfiore, A., et al. (2022). Fasting-Mimicking Diet Is Safe and Reshapes Metabolism and Antitumor Immunity in Patients with Cancer. Cancer Discov. *12*, 90–107. https://doi.org/10.1158/2159-8290.Cd-21-0030.
12. Ligorio, F., Fucà, G., Provenzano, L., Lobefaro, R., Zanenga, L., Vingiani, A., Belfiore, A., Lorenzoni, A., Alessi, A., Pruneri, G., et al. (2022). Exceptional tumour responses to fasting-mimicking diet combined with standard anticancer therapies: A sub-analysis of the NCT03340935 trial. Eur. J. Cancer *172*, 300–310. https://doi.org/10.1016/j.ejca.2022.05.046.
13. Ligorio, F., Lobefaro, R., Fucà, G., Provenzano, L., Zanenga, L., Nasca, V., Sposetti, C., Salvadori, G., Ficchì, A., Franza, A., et al. (2024). Adding fasting-mimicking diet to first-line carboplatin-based chemotherapy is associated with better overall survival in advanced triple-negative breast cancer patients: A subanalysis of the NCT03340935 trial. Int. J. Cancer *154*, 114–123. https://doi.org/10.1002/ijc.34701.
14. Elgendy, M., Cirò, M., Hosseini, A., Weiszmann, J., Mazzarella, L., Ferrari, E., Cazzoli, R., Curigliano, G., DeCensi, A., Bonanni, B., et al. (2019).

Combination of Hypoglycemia and Metformin Impairs Tumor Metabolic Plasticity and Growth by Modulating the PP2A-GSK3beta-MCL-1 Axis. Cancer Cell *35*, 798–815.e5. https://doi.org/10.1016/j.ccell.2019.03.007.

15. Schmid, P., Cortes, J., Pusztai, L., McArthur, H., Kümmel, S., Bergh, J., Denkert, C., Park, Y.H., Hui, R., Harbeck, N., et al. (2020). Pembrolizumab for Early Triple-Negative Breast Cancer. N. Engl. J. Med. *382*, 810–821. https://doi.org/10.1056/NEJMoa1910549.
16. Schmid, P., Cortes, J., Dent, R., Pusztai, L., McArthur, H., Kümmel, S., Bergh, J., Denkert, C., Park, Y.H., Hui, R., et al. (2022). Event-free Survival with Pembrolizumab in Early Triple-Negative Breast Cancer. N. Engl. J. Med. *386*, 556–567. https://doi.org/10.1056/NEJMoa2112651.
17. Alba, E., Chacon, J.I., Lluch, A., Anton, A., Estevez, L., Cirauqui, B., Carrasco, E., Calvo, L., Segui, M.A., Ribelles, N., et al. (2012). A randomized phase II trial of platinum salts in basal-like breast cancer patients in the neoadjuvant setting. Results from the GEICAM/2006-03, multicenter study. Breast Cancer Res. Treat. *136*, 487–493. https://doi.org/10.1007/s10549-012-2100-y.
18. von Minckwitz, G., Schneeweiss, A., Loibl, S., Salat, C., Denkert, C., Rezai, M., Blohmer, J.U., Jackisch, C., Paepke, S., Gerber, B., et al. (2014). Neoadjuvant carboplatin in patients with triple-negative and HER2-positive early breast cancer (GeparSixto; GBG 66): a randomised phase 2 trial. Lancet Oncol. *15*, 747–756. https://doi.org/10.1016/S1470-2045(14)70160-3.
19. Sikov, W.M., Berry, D.A., Perou, C.M., Singh, B., Cirrincione, C.T., Tolaney, S.M., Kuzma, C.S., Pluard, T.J., Somlo, G., Port, E.R., et al. (2015). Impact of the Addition of Carboplatin and/or Bevacizumab to Neoadjuvant Once-per-Week Paclitaxel Followed by Dose-Dense Doxorubicin and Cyclophosphamide on Pathologic Complete Response Rates in Stage II to III Triple-Negative Breast Cancer: CALGB 40603 (Alliance). J. Clin. Oncol. *33*, 13–21. https://doi.org/10.1200/JCO.2014.57.0572.
20. Ando, M., Yamauchi, H., Aogi, K., Shimizu, S., Iwata, H., Masuda, N., Yamamoto, N., Inoue, K., Ohono, S., Kuroi, K., et al. (2014). Randomized phase II study of weekly paclitaxel with and without carboplatin followed by cyclophosphamide/epirubicin/5-fluorouracil as neoadjuvant chemotherapy for stage II/IIIA breast cancer without HER2 overexpression. Breast Cancer Res. Treat. *145*, 401–409. https://doi.org/10.1007/s10549-014-2947-1.
21. Zhang, P., Yin, Y., Mo, H., Zhang, B., Wang, X., Li, Q., Yuan, P., Wang, J., Zheng, S., Cai, R., et al. (2016). Better pathologic complete response and relapse-free survival after carboplatin plus paclitaxel compared with epirubicin plus paclitaxel as neoadjuvant chemotherapy for locally advanced triple-negative breast cancer: a randomized phase 2 trial. Oncotarget *7*, 60647–60656. https://doi.org/10.18632/oncotarget.10607.
22. Loibl, S., O'Shaughnessy, J., Untch, M., Sikov, W.M., Rugo, H.S., McKee, M.D., Huober, J., Golshan, M., von Minckwitz, G., Maag, D., et al. (2018). Addition of the PARP inhibitor veliparib plus carboplatin or carboplatin alone to standard neoadjuvant chemotherapy in triple-negative breast cancer (BrighTNess): a randomised, phase 3 trial. Lancet Oncol. *19*, 497–509. https://doi.org/10.1016/S1470-2045(18)30111-6.
23. Schneeweiss, A., Möbus, V., Tesch, H., Hanusch, C., Denkert, C., Lübbe, K., Huober, J., Klare, P., Kümmel, S., Untch, M., et al. (2019). Intense dose-dense epirubicin, paclitaxel, cyclophosphamide versus weekly paclitaxel, liposomal doxorubicin (plus carboplatin in triple-negative breast cancer) for neoadjuvant treatment of high-risk early breast cancer (GeparOcto-GBG 84): A randomised phase III trial. Eur. J. Cancer *106*, 181–192. https://doi.org/10.1016/j.ejca.2018.10.015.
24. Lobefaro, R., Zattarin, E., Nichetti, F., Prisciandaro, M., Ligorio, F., Brambilla, M., Sepe, P., Corti, F., Peverelli, G., Ottini, A., et al. (2020). Antitumor activity and efficacy of shorter versus longer duration of anthracycline-taxane neoadjuvant chemotherapy in stage II–III HER2-negative breast cancer: a 10-year, retrospective analysis. Ther. Adv. Med. Oncol. *12*, 1758835920970081. https://doi.org/10.1177/1758835920970081.
25. Schneeweiss, A., Moebus, V., Tesch, H., Hanusch, C., Denkert, C., Luebbe, K., Huober, J.B., Klare, P., Kummel, S., Untch, M., et al. (2017). A randomised phase III trial comparing two dose-dense, dose-intensified approaches (EPC and PM(Cb)) for neoadjuvant treatment of patients with high-risk early breast cancer (GeparOcto). J. Clin. Oncol. *35*, 518. https://doi.org/10.1200/JCO.2017.35.15_suppl.518.
26. Perou, C.M., Sørlie, T., Eisen, M.B., van de Rijn, M., Jeffrey, S.S., Rees, C.A., Pollack, J.R., Ross, D.T., Johnsen, H., Akslen, L.A., et al. (2000). Molecular portraits of human breast tumours. Nature *406*, 747–752. https://doi.org/10.1038/35021093.
27. Lehmann, B.D., and Pietenpol, J.A. (2014). Identification and use of biomarkers in treatment strategies for triple-negative breast cancer subtypes. J. Pathol. *232*, 142–150. https://doi.org/10.1002/path.4280.
28. Lehmann, B.D., Bauer, J.A., Chen, X., Sanders, M.E., Chakravarthy, A.B., Shyr, Y., and Pietenpol, J.A. (2011). Identification of human triple-negative breast cancer subtypes and preclinical models for selection of targeted therapies. J. Clin. Invest. *121*, 2750–2767. https://doi.org/10.1172/jci45014.
29. Gong, Y., Ji, P., Yang, Y.S., Xie, S., Yu, T.J., Xiao, Y., Jin, M.L., Ma, D., Guo, L.W., Pei, Y.C., et al. (2021). Metabolic-Pathway-Based Subtyping of Triple-Negative Breast Cancer Reveals Potential Therapeutic Targets. Cell Metab. *33*, 51–64.e9. https://doi.org/10.1016/j.cmet.2020.10.012.
30. Charoentong, P., Finotello, F., Angelova, M., Mayer, C., Efremova, M., Rieder, D., Hackl, H., and Trajanoski, Z. (2017). Pan-cancer Immunogenomic Analyses Reveal Genotype-Immunophenotype Relationships and Predictors of Response to Checkpoint Blockade. Cell Rep. *18*, 248–262. https://doi.org/10.1016/j.celrep.2016.12.019.
31. Magbanua, M.J.M., Wolf, D.M., Yau, C., Davis, S.E., Crothers, J., Au, A., Haqq, C.M., Livasy, C., Rugo, H.S., et al.; I-SPY 1 TRIAL Investigators (2015). Serial expression analysis of breast tumors during neoadjuvant chemotherapy reveals changes in cell cycle and immune pathways associated with recurrence and response. Breast Cancer Res. *17*, 73. https://doi.org/10.1186/s13058-015-0582-3.
32. Tickle, T., Tirosh, I., Georgescu, C., Brown, M., and Haas, B. (2019). InferCNV of the Trinity CTAT Project (Klarman Cell Observatory, Broad Institute of MIT and Harvard). https://www.bioconductor.org/packages/release/bioc/html/infercnv.html.
33. Meng, Y.M., Jiang, X., Zhao, X., Meng, Q., Wu, S., Chen, Y., Kong, X., Qiu, X., Su, L., Huang, C., et al. (2021). Hexokinase 2-driven glycolysis in pericytes activates their contractility leading to tumor blood vessel abnormalities. Nat. Commun. *12*, 6011. https://doi.org/10.1038/s41467-021-26259-y.
34. Kumar, S., and Dikshit, M. (2019). Metabolic Insight of Neutrophils in Health and Disease. Front. Immunol. *10*, 2099. https://doi.org/10.3389/fimmu.2019.02099.
35. Cantelmo, A.R., Conradi, L.C., Brajic, A., Goveia, J., Kalucka, J., Pircher, A., Chaturvedi, P., Hol, J., Thienpont, B., Teuwen, L.A., et al. (2016). Inhibition of the Glycolytic Activator PFKFB3 in Endothelium Induces Tumor Vessel Normalization, Impairs Metastasis, and Improves Chemotherapy. Cancer Cell *30*, 968–985. https://doi.org/10.1016/j.ccell.2016.10.006.
36. Ozcan, M., Guo, Z., Valenzuela Ripoll, C., Diab, A., Picataggi, A., Rawnsley, D., Lotfinaghsh, A., Bergom, C., Szymanski, J., Hwang, D., et al. (2023). Sustained alternate-day fasting potentiates doxorubicin cardiotoxicity. Cell Metab. *35*, 928–942.e4. https://doi.org/10.1016/j.cmet.2023.02.006.
37. de Groot, S., Lugtenberg, R.T., Cohen, D., Welters, M.J.P., Ehsan, I., Vreeswijk, M.P.G., Smit, V.T.H.B.M., de Graaf, H., Heijns, J.B., Portielje, J.E.A., et al. (2020). Fasting mimicking diet as an adjunct to neoadjuvant chemotherapy for breast cancer in the multicentre randomized phase 2 DIRECT trial. Nat. Commun. *11*, 3083. https://doi.org/10.1038/s41467-020-16138-3.
38. Vernieri, C., Ligorio, F., Zattarin, E., Rivoltini, L., and de Braud, F. (2020). Fasting-mimicking diet plus chemotherapy in breast cancer treatment. Nat. Commun. *11*, 4274. https://doi.org/10.1038/s41467-020-18194-1.
39. Jordan, S., Tung, N., Casanova-Acebes, M., Chang, C., Cantoni, C., Zhang, D., Wirtz, T.H., Naik, S., Rose, S.A., Brocker, C.N., et al. (2019). Dietary Intake Regulates the Circulating Inflammatory Monocyte Pool. Cell *178*, 1102–1114.e17. https://doi.org/10.1016/j.cell.2019.07.050.

40. Li, W., Tanikawa, T., Kryczek, I., Xia, H., Li, G., Wu, K., Wei, S., Zhao, L., Vatan, L., Wen, B., et al. (2018). Aerobic Glycolysis Controls Myeloid-Derived Suppressor Cells and Tumor Immunity via a Specific CEBPB Isoform in Triple-Negative Breast Cancer. Cell Metab. *28*, 87–103.e6. https://doi.org/10.1016/j.cmet.2018.04.022.

41. Yu, P., Wilhelm, K., Dubrac, A., Tung, J.K., Alves, T.C., Fang, J.S., Xie, Y., Zhu, J., Chen, Z., De Smet, F., et al. (2017). FGF-dependent metabolic control of vascular development. Nature *545*, 224–228. https://doi.org/10.1038/nature22322.

42. Caccialanza, R., Aprile, G., Cereda, E., and Pedrazzoli, P. (2019). Fasting in oncology: a word of caution. Nat. Rev. Cancer *19*, 177. https://doi.org/10.1038/s41568-018-0098-0.

43. Heymsfield, S.B., Yang, S., McCarthy, C., Brown, J.B., Martin, C.K., Redman, L.M., Ravussin, E., Shen, W., Müller, M.J., and Bosy-Westphal, A. (2023). Proportion of caloric restriction-induced weight loss as skeletal muscle. Obesity (Silver Spring) *32*, 32–40. https://doi.org/10.1002/oby.23910.

44. Cazzoli, R., Romeo, F., Pallavicini, I., Peri, S., Romanenghi, M., Pérez-Valencia, J.A., Hagag, E., Ferrucci, F., Elgendy, M., Vittorio, O., et al. (2023). Endogenous PP2A inhibitor CIP2A degradation by chaperone-mediated autophagy contributes to the antitumor effect of mitochondrial complex I inhibition. Cell Rep. *42*, 112616. https://doi.org/10.1016/j.celrep.2023.112616.

45. Pusceddu, S., Vernieri, C., Di Maio, M., Marconcini, R., Spada, F., Massironi, S., Ibrahim, T., Brizzi, M.P., Campana, D., Faggiano, A., et al. (2018). Metformin Use Is Associated With Longer Progression-Free Survival of Patients With Diabetes and Pancreatic Neuroendocrine Tumors Receiving Everolimus and/or Somatostatin Analogues. Gastroenterology *155*, 479–489.e7. https://doi.org/10.1053/j.gastro.2018.04.010.

46. Pusceddu, S., Corti, F., Prinzi, N., Nichetti, F., Ljevar, S., Busico, A., Cascella, T., Leporati, R., Oldani, S., Pircher, C.C., et al. (2023). Safety and antitumor activity of metformin plus lanreotide in patients with advanced gastro-intestinal or lung neuroendocrine tumors: the phase Ib trial MetNET2. J. Hematol. Oncol. *16*, 119. https://doi.org/10.1186/s13045-023-01510-9.

47. Kordes, S., Pollak, M.N., Zwinderman, A.H., Mathôt, R.A., Weterman, M.J., Beeker, A., Punt, C.J., Richel, D.J., and Wilmink, J.W. (2015). Metformin in patients with advanced pancreatic cancer: a double-blind, randomised, placebo-controlled phase 2 trial. Lancet Oncol. *16*, 839–847. https://doi.org/10.1016/S1470-2045(15)00027-3.

48. Reni, M., Dugnani, E., Cereda, S., Belli, C., Balzano, G., Nicoletti, R., Liberati, D., Pasquale, V., Scavini, M., Maggiora, P., et al. (2016). (Ir)relevance of Metformin Treatment in Patients with Metastatic Pancreatic Cancer: An Open-Label, Randomized Phase II Trial. Clin. Cancer Res. *22*, 1076–1085. https://doi.org/10.1158/1078-0432.Ccr-15-1722.

49. Wen, J., Yi, Z., Chen, Y., Huang, J., Mao, X., Zhang, L., Zeng, Y., Cheng, Q., Ye, W., Liu, Z., et al. (2022). Efficacy of metformin therapy in patients with cancer: a meta-analysis of 22 randomised controlled trials. BMC Med. *20*, 402. https://doi.org/10.1186/s12916-022-02599-4.

50. Goodwin, P.J., Chen, B.E., Gelmon, K.A., Whelan, T.J., Ennis, M., Lemieux, J., Ligibel, J.A., Hershman, D.L., Mayer, I.A., Hobday, T.J., et al. (2022). Effect of Metformin vs Placebo on Invasive Disease-Free Survival in Patients With Breast Cancer: The MA.32 Randomized Clinical Trial. JAMA *327*, 1963–1973. https://doi.org/10.1001/jama.2022.6147.

51. Koppold, D.A., Breinlinger, C., Hanslian, E., Kessler, C., Cramer, H., Khokhar, A.R., Peterson, C.M., Tinsley, G., Vernieri, C., Bloomer, R.J., et al. (2024). International consensus on fasting terminology. Cell Metab. *36*, 1779–1794.e4. https://doi.org/10.1016/j.cmet.2024.06.013.

52. Wolff, A.C., Hammond, M.E.H., Hicks, D.G., Dowsett, M., McShane, L.M., Allison, K.H., Allred, D.C., Bartlett, J.M.S., Bilous, M., Fitzgibbons, P., et al. (2013). Recommendations for human epidermal growth factor receptor 2 testing in breast cancer: American Society of Clinical Oncology/College of American Pathologists clinical practice guideline update. J. Clin. Oncol. *31*, 3997–4013. https://doi.org/10.1200/jco.2013.50.9984.

53. Litton, J.K., Regan, M.M., Pusztai, L., Rugo, H.S., Tolaney, S.M., Garrett-Mayer, E., Amiri-Kordestani, L., Basho, R.K., Best, A.F., Boileau, J.F., et al. (2023). Standardized Definitions for Efficacy End Points in Neoadjuvant Breast Cancer Clinical Trials: NeoSTEEP. J. Clin. Oncol. *41*, 4433–4442. https://doi.org/10.1200/jco.23.00435.

54. Giuliano, A.E., Edge, S.B., and Hortobagyi, G.N. (2018). Eighth Edition of the AJCC Cancer Staging Manual: Breast cancer. Ann. Surg. Oncol. *25*, 1783–1785. https://doi.org/10.1245/s10434-018-6486-6.

55. Poggio, F., Bruzzone, M., Ceppi, M., Pondé, N.F., La Valle, G., Del Mastro, L., de Azambuja, E., and Lambertini, M. (2018). Platinum-based neoadjuvant chemotherapy in triple-negative breast cancer: a systematic review and meta-analysis. Ann. Oncol. *29*, 1497–1508. https://doi.org/10.1093/annonc/mdy127.

56. Simon, R. (1989). Optimal two-stage designs for phase II clinical trials. Control. Clin. Trials *10*, 1–10. https://doi.org/10.1016/0197-2456(89)90015-9.

57. Shen, W., Punyanitya, M., Wang, Z., Gallagher, D., St-Onge, M.P., Albu, J., Heymsfield, S.B., and Heshka, S. (2004). Total body skeletal muscle and adipose tissue volumes: estimation from a single abdominal cross-sectional image. J. Appl. Physiol. (1985) *97*, 2333–2338. https://doi.org/10.1152/japplphysiol.00744.2004.

58. Mourtzakis, M., Prado, C.M.M., Lieffers, J.R., Reiman, T., McCargar, L.J., and Baracos, V.E. (2008). A practical and precise approach to quantification of body composition in cancer patients using computed tomography images acquired during routine care. Appl. Physiol. Nutr. Metab. *33*, 997–1006. https://doi.org/10.1139/H08-075.

59. Korotkevich, G., Sukhov, V., Budin, N., Shpak, B., Artyomov, M.N., and Sergushichev, A. (2021). Fast gene set enrichment analysis. Preprint at bioRxiv. https://doi.org/10.1101/060012.

60. Hänzelmann, S., Castelo, R., and Guinney, J. (2013). GSVA: gene set variation analysis for microarray and RNA-seq data. BMC Bioinformatics *14*, 7. https://doi.org/10.1186/1471-2105-14-7.

61. Paquet, E., and Hallett, M. (2023). AIMS: Absolute Assignment of Breast Cancer Intrinsic Molecular Subtype. 10.18129/B9.bioc.AIMS.

62. Hao, Y., Stuart, T., Kowalski, M.H., Choudhary, S., Hoffman, P., Hartman, A., Srivastava, A., Molla, G., Madad, S., Fernandez-Granda, C., and Satija, R. (2024). Dictionary learning for integrative, multimodal and scalable single-cell analysis. Nat. Biotechnol. *42*, 293–304. https://doi.org/10.1038/s41587-023-01767-y.

63. Ewels, P.A., Peltzer, A., Fillinger, S., Patel, H., Alneberg, J., Wilm, A., Garcia, M.U., Di Tommaso, P., and Nahnsen, S. (2020). The nf-core framework for community-curated bioinformatics pipelines. Nat. Biotechnol. *38*, 276–278. https://doi.org/10.1038/s41587-020-0439-x.

64. Grüning, B., Dale, R., Sjödin, A., Chapman, B.A., Rowe, J., Tomkins-Tinch, C.H., Valieris, R., and Köster, J.; Bioconda Team (2018). Bioconda: sustainable and comprehensive software distribution for the life sciences. Nat. Methods *15*, 475–476. https://doi.org/10.1038/s41592-018-0046-7.

65. da Veiga Leprevost, F., Grüning, B.A., Alves Aflitos, S., Röst, H.L., Uszkoreit, J., Barsnes, H., Vaudel, M., Moreno, P., Gatto, L., Weber, J., et al. (2017). BioContainers: an open-source and community-driven framework for software standardization. Bioinformatics *33*, 2580–2582. https://doi.org/10.1093/bioinformatics/btx192.

66. Di Tommaso, P., Chatzou, M., Floden, E.W., Barja, P.P., Palumbo, E., and Notredame, C. (2017). Nextflow enables reproducible computational workflows. Nat. Biotechnol. *35*, 316–319. https://doi.org/10.1038/nbt.3820.

STAR★METHODS

KEY RESOURCES TABLE

REAGENT or RESOURCE	SOURCE	IDENTIFIER
Biological samples		
Patient blood samples	This paper, Fondazione IRCCS Istituto Nazionale dei Tumori di Milano	N/A
Patient tumor tissue samples	This paper, Fondazione IRCCS Istituto Nazionale dei Tumori di Milano	N/A
Chemicals, peptides, and recombinant proteins		
Liberase™	Roche, Besel, Switzerland	Cat# LIBTM-RO
TrypLE™ Express Enzyme (1X)	Thermo Fisher Scientific, Walthman, MA, USA	Cat# 12604013
ACK Lysing Buffer	Thermo Fisher Scientific, Walthman, MA, USA	Cat# A1049201
Gibco™ DMEM, high glucose, pyruvate	Thermo Fisher Scientific, Walthman, MA, USA	Cat# 11965092
Gibco™ DPBS, no calcium, no magnesium	Thermo Fisher Scientific, Walthman, MA, USA	Cat# 14190144
Estrogen Receptor antibody (EP1)	Agilent Technologies, Santa Clara, CA, USA	Cat# M3643
Progesterone Receptor antibody (PgR 636)	Agilent Technologies, Santa Clara, CA, USA	Cat# M3568
Ki-67 (MIB-1)	Agilent Technologies, Santa Clara, CA, USA	Cat# IS626
EnVision FLEX, High pH (Link)	Agilent Technologies, Santa Clara, CA, USA	Cat# K800021-2
Critical commercial assays		
RNeasy mini kit	Qiagen, Hilden, Germany	Cat# 74104
Agilent RNA 6000 Nano Kit	Agilent Technologies, Santa Clara, USA,	Cat# 5067-1511
Illumina Stranded Total RNA Prep with Ribo-Zero Plus	Illumina, San Diego, CA, USA	Cat# 20040529
Chromium Next GEM Single Cell 5' v2 kit	10X Genomics, Pleasanton, CA, USA	Cat#1000263
Deposited data		
Raw data (bulk RNA-seq data of BREAKFAST trial samples)	This paper	EGA: EGAD50000000968
Raw data (scRNA-seq data of BREAKFAST trial samples)	This paper	N/A
Raw data (bulk RNA-seq data of murine tumor specimens)	This paper	ArrayExpress: E-MTAB-14421
Source data (clinical data of patients in the BREAKFAST trial, INT 92/20 and INT 79/17 studies; metabolomics data, tumor volumes and survival data of mouse experiments)	This paper	Data S1
Transcriptomic data from the I-SPY1 trial	Magbanua et al.[31]	GEO: GSE32603
Human reference genome NCBI build 38, GRCh38	Genome Reference Consortium	http://www.ncbi.nlm.nih.gov/projects/genome/assembly/grc/human/
Mouse reference genome, GRCm39	Genome Reference Consortium	http://www.ncbi.nlm.nih.gov/projects/genome/assembly/grc/mouse/
Software and algorithms		
R software (version 4.3.1, or 4.3.2 when specified)	http://www.r-project.org/	RRID:SCR_001905
RStudio (v 2023.06.2+561)	http://www.r-project.org/	RRID:SCR_000432
Slice-O-Matic software v6.0	TomoVision, Montreal, Canada	N/A
nf-core/rnaseq pipeline (v 3.3)	https://zenodo.org/records/10471647	https://doi.org/10.5281/zenodo.1400710
DESeq2 (v1.42.0)	https://bioconductor.org/packages/release/bioc/html/DESeq2.html	RRID:SCR_015687

(*Continued on next page*)

Continued		
REAGENT or RESOURCE	SOURCE	IDENTIFIER
fgsea (v1.28.0)	https://bioconductor.org/packages/release/bioc/html/fgsea.html	RRID:SCR_020938
gsva (v1.50.0)	https://www.bioconductor.org/packages/release/bioc/html/GSVA.html	RRID:SCR_021058
GSEA Molecular Signatures Database	http://www.gsea-msigdb.org/gsea/msigdb/collections.jsp	N/A
EnrichR database	https://maayanlab.cloud/Enrichr/#libraries;	N/A
TNBCtype online subtyping tool	http://cbc.mc.vanderbilt.edu/tnbc/	N/A
Cellranger (v 7.1.0)	10x Genomics	RRID:SCR_023221
Seurat (v5.0.1)	http://seurat.r-forge.r-project.org/	RRID:SCR_007322
sctransform (v0.4.1)	https://github.com/satijalab/sctransform	RRID:SCR_022146
DoubletFinder (v 2.0.4)	https://github.com/chris-mcginnis-ucsf/DoubletFinder	RRID:SCR_018771
SingleR	https://www.bioconductor.org/packages/release/bioc/html/SingleR.html	RRID:SCR_023120
AUCell	https://bioconductor.org/packages/AUCell/	RRID:SCR_021327
harmony (v1.2.0)	https://github.com/immunogenomics/harmony	RRID:SCR_022206
inferCNV (v1.11.3)	https://www.bioconductor.org/packages/release/bioc/html/infercnv.html	RRID:SCR_021140
Xcalibur Quan Browser software and Compound Discoverer 3.3	Thermo Fisher Scientific, Walthman, MA, USA	N/A
Cell lines		
Mouse BALB/cfC3H: 4T1 cells	ATCC	CRL-2539
Experimental modes: Organism/strains		
Balbc olahsd	ENVIGO	N/A
Other		
CT scan images for body composition analysis	This paper, Fondazione IRCCS Istituto Nazionale dei Tumori di Milano	N/A

EXPERIMENTAL MODEL AND STUDY PARTICIPANT DETAILS

Study design and patients

The BREAKFAST (clinicaltrial.gov registration code: NCT04248998, see Methods S1 for study protocol) trial was a single center, open-label, two-arm, non-comparative, randomized phase 2 study that enrolled patients with treatment naïve, unilateral, localized (stage I-III, with clinical tumor diameter of at least 1 cm) invasive TNBC (negative HER2, ER, and PgR status according to American Society of Clinical Oncology/College of American Pathologists guidelines[52]). The study was conducted at Fondazione IRCCS Istituto Nazionale dei Tumori, Milan, Italy. All TNBC pathological diagnoses were centrally reviewed by two expert pathologists (A.V. and G. P.). Eligible patients were women aged between 18 and 75 years with Eastern Cooperative Oncology Group (ECOG) performance status of 0 or 1, adequate hematological, renal, and hepatic function; a BMI equal to or higher than 20 kg/m^2, and a LVEF of at least 50% at study enrollment. Patients were excluded if they had experienced significant, non-intentional weight loss during the 3 months before enrollment, if they had a diagnosis of type 1 or 2 diabetes mellitus requiring pharmacologic therapy, or if they had clinically relevant gastrointestinal diseases. Clinical T stage was defined by the longest tumor diameter measured by breast Magnetic Resonance Imaging (MRI) before the initiation of the neoadjuvant treatment.

All patients enrolled in the BREAKFAST trial received preoperative chemotherapy, consisting of 4 triweekly cycles of intravenous doxorubicin (60 mg/m^2) plus cyclophosphamide (600 mg/m^2), followed by 12 cycles of weekly intravenous paclitaxel (80 mg/m^2). At enrollment, patients were randomized in a 1:1 fashion to receive additional treatment in one of the two experimental arms: triweekly 5-day FMD, up to a maximum of 8 consecutive cycles (arm A); triweekly 5-day FMD, up to a maximum of 8 consecutive cycles, in combination with daily oral metformin at a daily dosage of 850 mg for the first 21 days and, subsequently, at a daily dosage of 1700 mg. Tumor stage and patient BMI were used as stratification factors at randomization. Cyclic FMD consisted of a plant-based, low-calorie (about 600 Kcal on day 1; about 300 Kcal on days 2 to 5), low-protein, low-carbohydrate dietary intervention lasting 5 days, as previously described.[11] No modifications nor personalization of the prescribed FMD regimen were allowed. Each FMD cycle was repeated every three-weeks, except for patients who delayed chemotherapy administration because of occurring AEs, or of patients who were unable to reach a minimum BMI of 20 kg/m^2 at the time of the initiation of the subsequent FMD cycle.

The FMD started two days prior to the day of chemotherapy administration and it continued for additional three days (including the day of chemotherapy administration). After completion of the experimental preoperative protocol, patients underwent surgery between 14 and 28 days after the last chemotherapy administration. In case of residual disease at the pathological examination, patients may have received adjuvant systemic treatment as per clinical practice. After surgery, patients could receive local radiotherapy, depending on pathological stage, and according to local and international guidelines. AEs occurring during each FMD cycle were collected from patient daily reports. The following AEs were attributed to the FMD if they occurred during the 5-day nutritional intervention: fatigue, headache, insomnia, somnolence, constipation, muscle cramps, dizziness, nausea, vomiting, syncope, presyncope, epigastric pain, hot flushes, tremor, hypoglycemia. The following biochemical alterations were also considered to be FMD-related AEs: increased concentration of blood cholesterol, triglycerides, uric acid, aspartate aminotransferase (AST), alanine aminotransferase (ALT) or creatinine levels. AEs were graded according to the Common Terminology Criteria for Adverse Events (CTCAE), Version 5.0 (https://evs.nci.nih.gov/ftp1/CTCAE/CTCAE_5.0).

The BREAKFAST trial was conducted in accordance with Good Clinical Practice guidelines and the provisions of the Declaration of Helsinki. Protocol approval was obtained from the Institutional Review Board (IRB) and the Ethics Committee of Fondazione IRCCS Istituto Nazionale dei Tumori di Milano (INT 192/19). All patients provided written informed consent for enrollment before any study-related procedures, as well as for the use of clinical and biological data for research purposes.

INT 79/17 trial

As a control cohort for the evaluation of LDH plasmatic levels before and after chemotherapy alone, we included patients enrolled in the observational prospective INT79/17 study, which evaluated biomarkers of response to carboplatin plus gemcitabine chemotherapy in advanced TNBC patients, as previously described.[11]

INT 92/20 study

As a control cohort to evaluate tumor pCR rates according to baseline BMI and to study LVEF changes during the study treatment, we used an independent retrospective cohort of early-stage TNBC patients treated with anthracycline-taxane-based neoadjuvant chemotherapy alone at our Institution between October 2007 and January 2018 (n=76) (Table S3). Echocardiography data were available for 33 of these patients. The collection of clinical data from these patients was performed as part of a retrospective observational study (INT 92/20) approved by the Ethics Committee of Fondazione IRCCS Istituto Nazionale dei Tumori. Patients alive at the time of data collection and/or analysis signed an informed consent for the use of their personal data for research purposes.

Public transcriptomic data from the I-SPY-1 trial

As a control cohort for bulk transcriptomic analyses, we employed publicly available gene expression data from 12 matched early-stage TNBC samples collected in the context of the I-SPY1 trial. Tumor biopsies were collected before treatment initiation (T0), and between 24 and 96 hours after the first dose (T1) of anthracycline-based neoadjuvant chemotherapy.[31]

Mouse models

Experiments involving animals were performed in accordance with the Italian Laws (D.lgs. 26/2014), which enforce Directive 2010/63/EU (Directive 2010/63/EU of the European Parliament and of the Council of 22 September 2010 on the protection of animals used for scientific purposes). All the experiments were approved by the Italian Ministry of Health. Animals were housed under specific pathogen-free conditions at 22 ± 2 °C and 55 ± 10% relative humidity, with 12 hours day/light cycles. 7-week-old female BALB/c/Ola Hsd mice (Envigo) were injected in the mammary fat pad with $2x10^4$ 4T1-luc (luciferase-positive) TNBC cells resuspended in 20 μl of medium (RPMI supplemented with 10% FBS, 2mM glutamine). When tumors became palpable (approximately 7 days after cells), mice were randomly assigned to *ad libitum* diet (control arm) or cyclic fasting (experimental arm). Tumor volumes were measured twice a week through a digital caliper according to the following equation: tumor volume (mm3) = length x width x thickness x 0,5. At the end of the experiments, mice were euthanized by using CO_2.

Animal diets

Mice were fed *ad libitum* with irradiated standard diet VRFI (P) diet (Charles River) containing 3,89 kcal/g of gross energy. According to the experimental groups, some mice were subjected to fasting once per week, consisting of 48-hour water-only-fasting, followed by 5 days of *ad libitum* refeeding (standard diet). Mouse weight was monitored twice per week and during any fasting cycle. In the experiments, weight loss could not exceed 20% as compared to baseline values. Before initiating a new fasting cycle, the animals should have completely recovered their original bodyweight.

METHOD DETAILS

Study endpoints

The primary study endpoint of the BREAKFAST trial was pCR, as defined as the absence of residual invasive disease on evaluation of surgical breast specimen and surgically-resected lymph nodes (i.e., ypT0/is ypN0 per the American Joint Committee on Cancer staging system[53,54]). In detail, we investigated if one or both experimental treatments, consisting in the combination of anthracycline-taxane chemotherapy with cyclic FMD, alone (Arm A) or in combination with daily metformin (Arm B), were able to increase the rate of

pCR when compared to historical results with anthracycline-taxane chemotherapy alone. Secondary study endpoints included: a) patient compliance to the experimental treatment; b) safety, which was measured as the incidence, nature and seriousness of AEs; all AEs were graded according to the CTCAE, Version 5.0; c) RFS, as defined as the time from surgery to disease recurrence (either local or distant) or death, whichever occurred first; d) DMFS, as defined as the time from surgery to distant recurrence or death: OS, as defined as the time from randomization to death for any cause. We also evaluated EFS, as defined as the time between randomization and disease progression that precluded definitive surgery, tumor recurrence (either local or distant), occurrence of a second primary cancer or death, whichever occurred first. Pre-planned exploratory analyses included metabolomics analyses, which were performed in blood samples, and transcriptomic analyses, which were performed at both bulk and single cell levels to study the modulation of genes and pathways involved in glucose metabolism, mitochondrial OXPHOS, TCA cycle, fatty acid and cholesterol metabolism, amino acid and nucleotide synthesis or catabolism.

FMD management and analysis of patient compliance

To promote patient compliance with the FMD and to monitor FMD tolerability, we ensured a daily contact between patients and a dedicated nutritionist involved in the BREAKFAST trial during each of the five days of each FMD cycle. This contact was crucial to communicate detailed information regarding the type and amount of foods and beverages consumed by patients, as well as updated weight and blood pressure measurements. In addition, during each 5-day FMD cycle, a physician involved in the study was available 24 hours a day to manage any emergent AE of clinical significance. Food diaries were analyzed to evaluate patient compliance, which was defined through the assessment of minor and major deviations from the prescribed dietary intervention. Minor deviations were defined as the consumption of foods and/or beverages allowed by the FMD scheme, but exceeding by 10-50% the total, daily caloric intake permitted as per protocol. Major deviations were defined as the consumption of any foods/beverages not present in the provided FMD scheme, regardless of its calorie content, or the consumption of allowed foods exceeding by 50% or more the permitted daily calorie intake. Two minor deviations occurring during the same FMD cycle were considered as a major deviation. Patients undergoing minor or major deviation during at least one day of a FMD cycle were defined as non-compliant during the whole FMD cycle.[11] We summarized compliance results by providing data about a) the proportion of patients who were compliant during the whole study, b) the percentage of individual FMD cycles completed with full patient adherence to the FMD. During the refeeding periods (i.e., in the days between FMD cycles), patients were advised to adhere to International Guidelines for Cancer Prevention and Cancer Survivors (https://www.wcrf.org/diet-activity-and-cancer/cancer-prevention-recommendations/after-a-cancer-diagnosis-follow-our-recommendations-if-you-can/; https://www.cancer.org/cancer/risk-prevention/diet-physical-activity/acs-guidelines-nutrition-physical-activity-cancer-prevention/guidelines.html; https://cancer-code-europe.iarc.fr.)

Sample size calculation

Based on a retrospective analysis of the available literature, the pCR rate associated with neoadjuvant anthracycline-taxane-based chemotherapy in patients with TNBC was assumed to be 45%, namely the upper limit of pCR rates reported with anthracycline-taxane-based neoadjuvant chemotherapy without carboplatin or immunotherapy.[55] The BREAKFAST trial was designed with the hypothesis that one or both experimental treatments are able to improve the pCR from 45% to 65%. A Simon's minimax, one-sample, two-stage testing procedure[56] was separately applied to each of the two treatment arms with the following hypotheses: a pCR in 45% or fewer of patients was considered insufficient to warrant additional investigation (i.e., p0=45%), while a pCR in 65% or more than 65% of patients in at least one of the experimental arms was considered sufficient to warrant additional investigation of that particular treatment regimen (i.e., p1=65%). The application of these hypotheses with type I and type II errors of 10% each ($\alpha = \beta = 0.10$) implied that, in the first stage, a total of 21 patients per cohort were needed and that if among them at least 10 pCR events had been observed, the accrual for that experimental arm would have continued until the achievement of a total of 41 patients. If at least 23 of these 41 patients (56%) had achieved pCR after treatment completion, then the study would have met its primary endpoint, and that treatment regimen would have warranted additional investigation. To correct patient drop-out (estimated as 5%), a surplus recruitment to a maximum of four patients was allowed. Therefore, we initially planned to enroll a total of 90 patients. Allocation of a patient to each treatment arm was based on a randomization list.

QUANTIFICATION AND STATISTICAL ANALYSIS

Statistical analysis

For descriptive analyses, the median and interquartile range (IQR) were reported for continuous variables, while categorical variables were summarized as percentages. The Pearson's chi-squared test was used to study the distribution of categorical variables (tumor or patient characteristics, adverse events, compliance) in patients in the two treatment arms, while the

Wilcoxon rank sum test was used to compare the distribution of continuous variables in the two treatment groups, as appropriate. The Pearson's chi-squared test was also used to compare pCR rates in patients with high or low BMI. The association between clinical and biological variables (LDH delta, dichotomized according to its mean value (high vs. low); Ki-67, as a continuous variable (OR refers to a 10% increase of Ki-67); tumor size, $\geq$T2 vs. T1; nodal status, positive vs. negative; treatment arm, arm B vs. arm A; gene expression and pathway activity (as continuous variables)), and the rate of pCR was assessed using univariate or multivariable logistic regression models. Correlations between BMI and body composition parameters were performed by Spearman's correlation. Paired Wilcoxon test was used to assess treatment-induced modulations of blood and urine metabolic parameters, intratumor

pathways GSVA ES or transcript expression levels, as well as changes in BMI and body composition parameters before vs. after treatment. Unpaired Wilcoxon test was used to compare LDH level modulation in patients achieving vs. not achieving pCR. BMI, body composition parameters, metabolic blood and urinary parameters, expression of genes of interest, and pathway activities (as GSVA ESs) were illustrated through box plots showing median values, with the boundaries of the rectangle representing the first and third quartiles. A significance threshold of 0.05 was used for all statistical tests. The P value for the indicated statistical test is reported for each comparison in each figure. All statistical analyses and graphs were performed with the software R version 4.3.1, RStudio (version 2023.06.2+561). All statistical tests that were performed were two-tailed.

Biological evaluations in blood samples

Standard laboratory assessments (hematology and/or clinical chemistry) were performed as per clinical practice. Additional assessments (metabolomic and immunological analyses) were performed on blood and urine samples collected at pre-specified timepoints (i.e., before and after the first, the second and the fifth FMD cycles, and at surgery) after at least 8-hour of complete fasting on the morning of FMD initiation (day 1) and on the morning of FMD completion (day 6), i.e., just before re-starting the normal diet. Here we reported data about plasma glucose, serum insulin, IGF-1 and LDH, and urinary ketone bodies.

BMI and body composition analysis

Patient weight was measured at the time of patient enrollment in the study. During treatment, patient weight was measured on day 1 (i.e., before FMD initiation) and on day 6 (i.e., before refeeding) of each FMD cycle, and before surgery. BMI was calculated at each timepoint as weight [kg]/(height[m]^2).

CT image analysis, an accurate technique to assess body composition both in healthy individuals[57] and oncologic patients,[58] was performed to estimate whole-body volumes of muscle and adipose tissue. Routinely acquired CT scans at diagnosis (T0), i.e., within 1 month from the first cycle of FMD, before surgery (T2), i.e., within 1 month after the last cycle of FMD, and 3 to 12 months after surgery (median time from surgery: 216.0 days, IQR range 164-337) (T3) were collected for each patient. A trained researcher (C.S.), using Slice-O-Matic software v6.0 (TomoVision, Montreal, Canada), quantified skeletal muscle cross-sectional area (SMA) and intermuscular adipose tissue (IMAT), VAT and SAT cross-sectional areas in centimeters squared from a single axial CT scan at the 3rd lumbar vertebrae (L3) level. Each area was computed based on tissue-specific Hounsfield Units (HU) ranges: -29 to +150 for skeletal muscle, -190 to -30 for subcutaneous and intermuscular adipose tissue, -150 to -50 to for visceral adipose tissue. SMI, which reflects whole-body muscle mass of each patient, was calculated as SMA divided for squared height in meter. TAT area was determined as the sum of IMAT, VAT and SAT.

Bulk RNA sequencing analysis (BREAKFAST trial)

Tumor samples collected through core biopsy procedures performed at baseline (T0) and after the first experimental treatment cycle (T1) were frozen soon after collection. Tumor specimens were evaluated by two expert pathologists (A.V. and G.P.). Briefly, prior to RNA extraction, biopsies were included in OCT and tissue sections were cut at cryostat. Frozen sections were stained with H&E and microscopically assessed for tumor cellularity. Samples with 70% or more of tumor content were entirely processed for RNA extraction, while samples with lesser tumor content were enriched by macrodissection. Cellular RNA was extracted using the RNeasy mini kit (Qiagen, Hilden, Germany, Cat# 74104) following manufacturer's instructions. RNA quality was evaluated using Agilent RNA 6000 Nano Kit (Agilent Technologies, Santa Clara, USA, Cat# 5067-1511) on the Agilent 2100 Bioanalyzer (Agilent Technologies, Santa Clara, USA). RNA sequencing libraries were prepared using Illumina Stranded Total RNA Prep with Ribo-Zero Plus (Illumina, San Diego, CA, USA, Cat# 20020598) according to the manufacturer's protocol and sequenced using 75nt paired end-sequencing on Illumina Nextseq 550 DX platform (Illumina, San Diego, CA, USA). RNA-seq reads were aligned to the GRCh38/hg38 assembly human reference genome using the nf-core/rnaseq pipeline (https://doi.org/10.5281/zenodo.1400710, version 3.3).

Differential gene expression (DEG) analysis comparing T1 vs. T0 samples was performed in an R environment using negative binomial distribution and Benjamini-Hochberg (B-H) FDR with the Bioconductor package DESeq2 (v1.42.0). Differences in the expression of individual genes between T1 and T0 were also studied comparing variance stabilizing transformed (vst), normalized gene expression data through paired Wilcoxon-test. Pathway-level analyses were performed by means of preranked GSEA using the Bioconductor package fgsea (v1.28.0),[59] and through GSVA using the Bioconductor package gsva (v1.50.0),[60] taking advantage of the KEGG, HALLMARK and Reactome gene sets available from the GSEA Molecular Signatures Database (http://www.gsea-msigdb.org/gsea/msigdb/collections.jsp; HALLMARK, Reactome) and EnrichR database (https://maayanlab.cloud/Enrichr/#libraries; KEGG). GSEA[59] was performed on genes ranked by the absolute value of $\log_{10}$(Pvalue) scaled by the sign of $\log_2$(FC) tested against gene lists of interest. To estimate the activity of pathways of interest at a single sample level GSVA[60] was performed; enrichment scores (ESs) were calculated on vst- normalized gene expression data. Differences in GSVA ESs between T1 and T0 samples were determined by the paired Wilcoxon-test. Pathways undergoing modifications passing the significance cut-off ($p < 0.05$, Benjamini-Hochberg FDR <0.1) were visually represented in a heatmap (Figure 4B). Intrinsic subtype classification of each baseline sample was performed using the AIMS method (v1.34.0).[61] To identify Lehmann TNBC subtypes[28] the TNBCtype online subtyping tool (http://cbc.mc.vanderbilt.edu/tnbc/) was used. Metabolic classification was performed through unsupervised k-means clustering based on the GSVA enrichment scores of KEGG metabolic pathways.[29] Cell type enrichment analysis from gene expression data was performed according to a set of pan-cancer metagenes for 28 immune cell sub-populations[30] as previously described.[11] All these analyses were performed with the software R version 4.3.1, RStudio (version 2023.06.2+561)

scRNA sequencing analysis (BREAKFAST trial)

For scRNA-seq analyses we collected fresh tumor samples at prespecified timepoints from 15 patients enrolled in the trial, finally obtaining scRNA-seq data from n=13 samples collected before treatment initiation (T0), n=11 samples collected after one treatment cycle (T1), and from n=5 samples collected at surgery (T2). Dedicated personnel (A.B., A.B., S.B.) promptly transferred fresh tumor tissue to the lab for immediate sample processing to obtain viable single cell suspensions. Briefly, fresh tumor was minced into cubes <1mm^3 and digested using Liberase™ (Roche, Besel, Switzerland) and TrypLE™ Express Enzyme (Thermo Fisher Scientific, Waltham, MA, USA). After filtration and centrifugation, the obtained cell pellet was resuspended in PBS + 0.04% BSA at 1000 cells/μL. Cancer cell viability was microscopically assessed by Trypan blue staining. Single cell suspensions were diluted (cell number target: 10.000 per sample), loaded on a Chromium Single Cell 5' Chip (10X Genomics) and run in the Chromium Controller of the 10x Genomics Chromium X platform to generate single cell gel beads emulsions, following manufacturer's instructions. Obtained libraries were sequenced on Illumina NovaSeq 6000 platform.

Cellranger v 7.1.0 has been used to demultiplex FASTQ files output and perform alignment, filtering, barcode and UMI counting to obtain feature and barcode count matrices. The following steps have been performed using a modified version of Satja's lab Seurat v5.0.1 pipeline[62] in R software version 4.3.1. To ensure high-quality data analysis, low-quality cells identified by the low number of expressed genes (<200) or high mitochondrial gene content (higher than 10% of the whole expression) have been filtered out. Similarly, lowly expressed genes (in less than 3 cells) have been removed. Cells expressing any amount (higher than 0.1% of the whole expression) of the following genes: *HBA1, HBA2, HBB, HBD, HBG2, HBM, AHSP, PPBP*, and *PF4* were removed to avoid erythrocytes and platelets contamination. Normalization and integration steps were carried out following the *sctransform* v0.4.1 R package pipeline. DoubletFinder v 2.0.4 has been used to remove doublets, whose estimates were computed according to the proportions outlined by the manufacturer. The integration was performed with *harmony* v1.2.0 R package, using the 5000 most variable genes in each dataset (SelectIntegrationFeatures function). The dimensionality of the data was calculated using the Elbow method, which determines 26 as the optimal number of dimensions to represent the dataset variability. Cell clusters were determined using Uniform Manifold Approximation and Projection (UMAP), a technique allowing non-linear dimension reduction run under Seurat function *findClusters*. We preliminarily annotated cell clusters using the *SingleR* package and the HumanPrimaryCellAtlas data. To reduce classification biases induced by ''pan-cell-atlas'' approaches, we subsequently proceeded to refine the classification using known cellular markers using the *AUCell* R package. To identify putative cancer cells, we assessed chromosomal changes in epithelial and myoepithelial cells with the inferCNV package (v1.11.3), using stromal cells and lymphocytes as a reference. To evaluate transcriptomic modulations across different conditions, we employed GSVA, thus allowing the estimation of gene set activity at the single-cell level. We calculated single-cell enrichment scores for predefined metabolic gene sets, and then subjected to statistical analysis to ascertain significant differences (adj p-value < 0,05; log2FC >0,25 or <-0.25) in gene set activity, providing insights into the modification induced by systemic treatment.

Bulk RNA sequencing analysis (murine 4T1 tumor specimens)

Total RNA was extracted from snap-frozen tumor masses collected after the second cycle of fasting, or at the corresponding timepoint in the control group, using the RNeasy Mini Kit (Cat. No 74104, QIAGEN).

The abundance and integrity of extracted RNA was assessed using Qubit fluorimeter an Agilent Bioanalyzer 2100 instrument (Agilent Technologies, Palo Alto, CA). For each sample, 500 ng of total RNA were used to generate a library of fragments using Illumina Stranded mRNA prep ligation kit. Oligo(dT) magnetic beads purified and captured mRNA molecules containing poly(A) tails. Then, purified mRNA was fragmented and copied into first strand complimentary DNA (cDNA) using reverse transcriptase and random primers. In a second strand cDNA synthesis step, dUTP replaced dTTP to achieve strand specificity. The final steps added adenine and thymine bases to fragment ends and ligated adapters. The resulting products were purified and selectively amplified with 12 cycles of PCR to generate an indexed library of fragments. The library was quantified using Qubit 4.0 fluorimeter, checked on Agilent Bioanalyzer 2100 then loaded on Illumina NextSeq550Dx sequencer for sequencing, following the manufacturer's instructions.

Library fragments were sequenced using 2x75nt read mode, thus sequencing 75 nucleotides from both ends of each fragment; on average, approximately 50 million paired-end fragments were sequenced for each sample. Sequencing results were generated in fastq.gz format.

RNA sequencing was performed at the Cogentech sequencing facility, Genomic Unit, Milan (Italy). RNAseq data were processed using nf-core/rnaseq v3.14.0 (doi: https://doi.org/10.5281/zenodo.1400710) of the nf-core workflow collection[63] using reproducible software environment from the Bioconda[64] and Biocontainers[65] projects. The pipeline was executed with Nextflow v23.10.0,[66] performing STAR-Salmon alignment-quantification and specifying the options ''gencode true'', ''gtf_group_features gene_name'', ''quantMode TranscriptomeSAM''. RNA sequencing data were aligned to the GRCm39 genome (Mus_musculus.GRCm39.dna.primary_assembly.fa). The gene-level length-scaled counts were used for downstream analyses. Gene-level length-scaled counts were used with the ''DESeq2'' R package (v1.42.0) for quality checks, including principal component analysis (PCA), and for differential expression analysis (comparing the group treated with fasting with the control group). Genes with low expression levels were filtered out, keeping only those with a total count of at least 5 for a minimum of 6 samples. Normalization was performed using variance stabilizing transformation [VST; function vst() from the DESeq2 R package].

One sample from the control group resulted an outlier at PCA on VST normalized data (including the top 500 most variable genes) and excluded from further analyses.

For gene set enrichment analysis (GSEA), genes were ranked using the "stat" column (Wald statistic) from the DESeq2 results. GSEA was performed using the "fgsea" R package (v1.28.0) on Hallmark (v2023.2, obtained from MSigDB mouse collections at https://www.gsea-msigdb.org/gsea/msigdb/) and Kyoto Encyclopedia of Genes and Genomes (KEGG) gene sets (obtained from the MSigDB with the "msigdbr" R package (v7.5.1, specifying species = "Mus musculus"). Pathways were considered significantly enriched for false discovery rates (FDRs)<0.05. These analyses were performed using R version 4.3.2.

Metabolomics analysis in murine plasma and tumor tissue

Metabolites were isolated with ice-cold extraction buffer (40% Acetonitrile, 40% Methanol, and 20% H_2O. 400ul of extraction buffer for 40ul of plasma; 25ul of extraction buffer/mg of tissue). Plasma samples were incubated at -20 degrees for 30 minutes, mixed for 15 minutes in a thermomixer at 4 degrees at 2000 rpm and centrifuged at 4 degrees for 20 minutes at maximum speed ($\geq$13000 rpm). The supernatant was transferred into autosampler vials (Waters #186000384C). Tumor samples were lysed by using PowerLyzer 24 homogenizer and zirconium beads (at 4 degrees) until complete disruption (2 or 3 cycle of 30 seconds each at 2000 rpm). Tumor samples were incubated at -20 degrees for 60 minutes, mixed for 15 minutes in a thermomixer at 4 degrees at 2000 rpm and centrifuged at 4 degrees for 15 minutes at maximum speed ($\geq$13000 rpm). The supernatant was transferred into autosampler vials (Waters #186000384C).

Analyses were performed using a UHPLC Vanquish Flex coupled to an Exploris 240 mass spectrometer (Thermo Fisher, Bremen, Germany). Five microliters of each sample were injected onto a Sequant ZIC-pHILIC column (150 x 2.1 mm, 5 μm) and guard column (20 x 2.1 mm, 5 μm) (both Merck Millipore) for chromatographic separation. Briefly, the mobile phase was composed of 20 mM ammonium carbonate and 0.2% ammonium hydroxide in water (mobile phase A), and acetonitrile (mobile phase B). The flow rate was set at 0.2 mL/min with the following gradient: 80% B for 2 minutes, linear decrease to 30% of B for 15 minutes, and then solvents were brought back to starting conditions and kept for 6 minutes. The column oven temperature was maintained at 40 °C for the entire run. The mass spectrometer was operated in Full MS and ddMS2 with the following parameters: mass range of 70-900m/z with polarity switching mode, 60000 of resolution for full MS and 30000 resolution for the ddMS2, normalized collision energies were set to 20, 40, and 80 values, AGC target and maximum injection time were set respectively to standard and auto for both full MS and ddMS2 scan. Metabolites were identified using acquired fragmentation spectra matched with online libraries and standard injections. Metabolites were quantified using Xcalibur Quan Browser software and Compound Discoverer 3.3 (Thermo Fisher). Metabolite intensities were normalized by either total ion count (TIC) or internal standard intensities.

ADDITIONAL RESOURCES

Clinical trial registration number and URL: NCT04248998, https://clinicaltrials.gov/study/NCT04248998

Cell Metabolism, Volume *37*

Supplemental information

Early downmodulation of tumor glycolysis predicts response to fasting-mimicking diet in triple-negative breast cancer patients

Francesca Ligorio, Andrea Vingiani, Tommaso Torelli, Caterina Sposetti, Lorenzo Drufuca, Fabio Iannelli, Lucrezia Zanenga, Catherine Depretto, Secondo Folli, Gianfranco Scaperrotta, Giuseppe Capri, Giulia V. Bianchi, Cristina Ferraris, Gabriele Martelli, Ilaria Maugeri, Leonardo Provenzano, Federico Nichetti, Luca Agnelli, Riccardo Lobefaro, Giovanni Fucà, Giuseppe Fotia, Luigi Mariani, Daniele Morelli, Vito Ladisa, Maria Carmen De Santis, Laura Lozza, Giovanna Trecate, Antonino Belfiore, Silvia Brich, Alessia Bertolotti, Daniele Lorenzini, Angela Ficchì, Antonia Martinetti, Elisa Sottotetti, Alessio Arata, Paola Corsetto, Luca Sorrentino, Mattia Rediti, Giulia Salvadori, Saverio Minucci, Marco Foiani, Giovanni Apolone, Massimiliano Pagani, Giancarlo Pruneri, Filippo de Braud, and Claudio Vernieri

SUPPLEMENTAL DOCUMENT 1

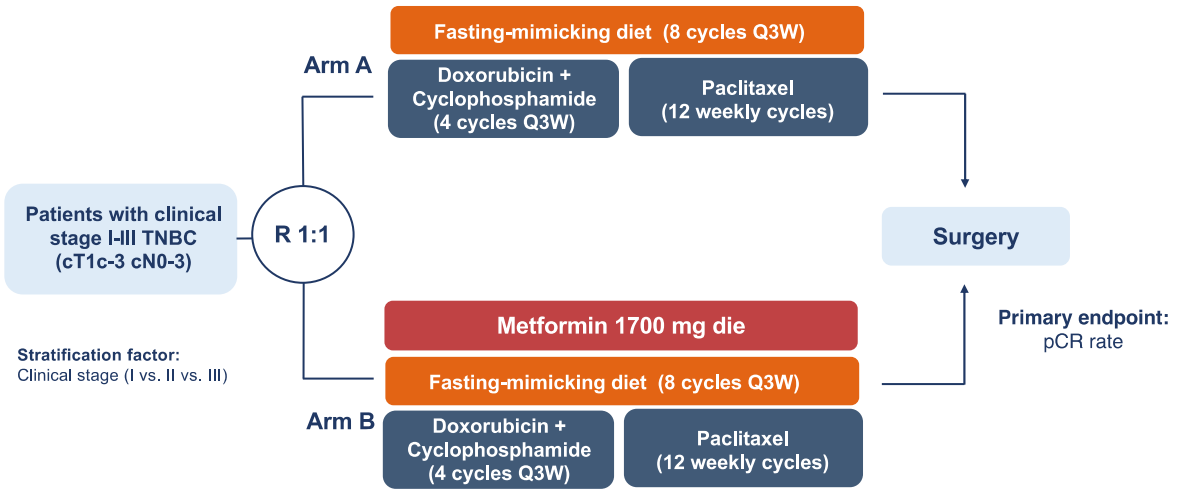

Figure S1, related to Figure 1. Study design. BREAKFAST is randomized, phase II trial that enrolled patients with stage I-III TNBC. Enrolled patients (n=30) received preoperative chemotherapy, which consisted of 4 triweekly cycles of intravenous doxorubicin (60 mg/m^2) plus cyclophosphamide (600 mg/m^2), followed by 12 cycles of weekly intravenous paclitaxel (80 mg/m^2). In addition to chemotherapy, patients were randomized in a 1:1 ratio to receive triweekly 5-day FMD up to a maximum of eight consecutive FMD cycles (arm A), or triweekly 5-day FMD in combination with daily oral metformin (up to a maximum daily dosage of 1700 mg). Disease stage and patient BMI were used as stratification factors at randomization. The primary study endpoint was the pCR rate. *TNBC: Triple Negative Breast Cancer*.

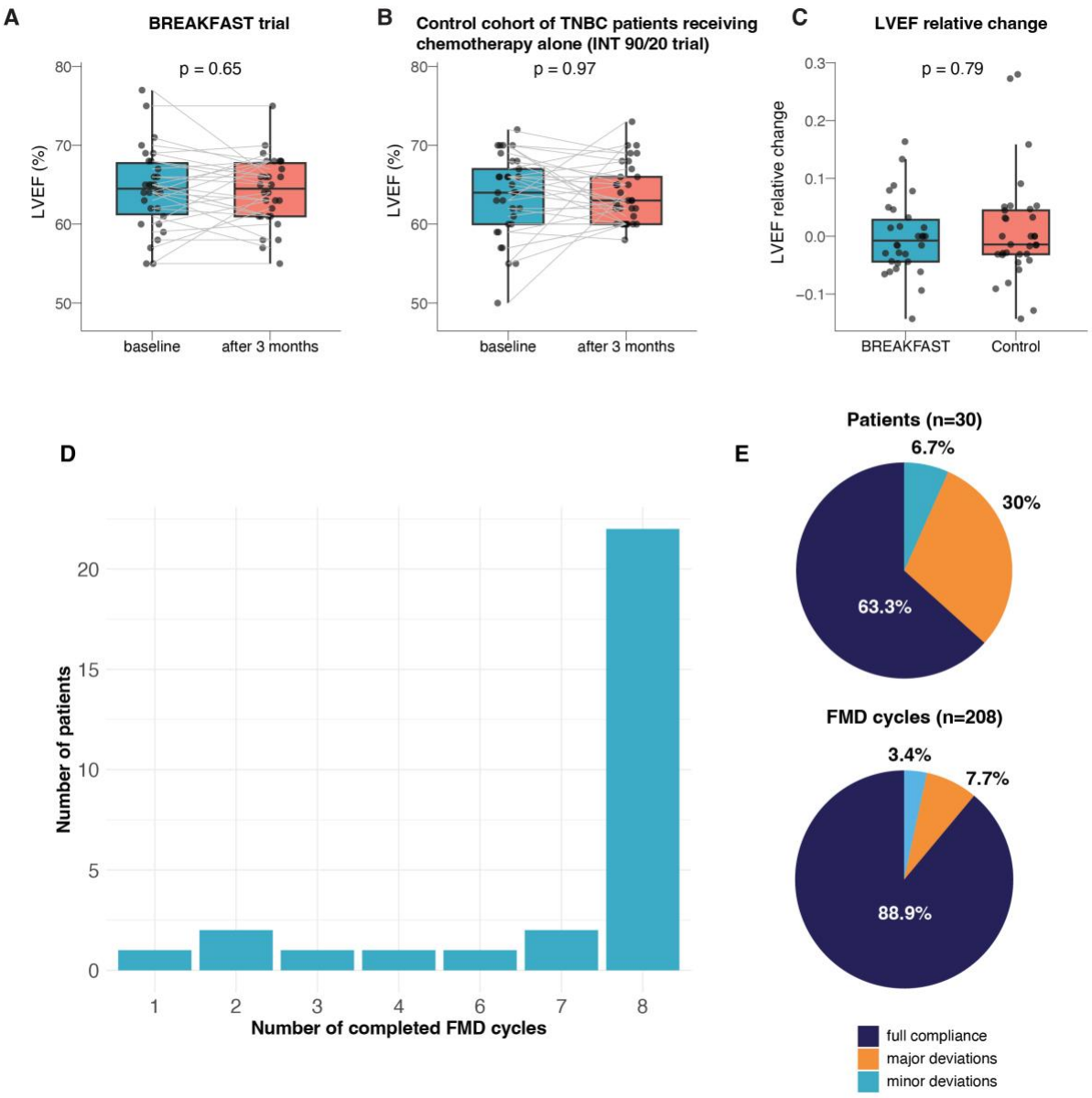

Figure S2 related to Table 1. Cardiac safety and patient compliance. (A and **B)** Boxplots showing LVEF at baseline and after about three months of anthracycline-based chemotherapy **(A)** in the BREAKFAST trial and **(B)** in a retrospective independent control cohort of n=33 patients with TNBC treated with neoadjuvant anthracycline-based chemotherapy alone in our Institution (INT 92/20 cohort). **(C)** Boxplots comparing relative LVEF changes (deltas) during anthracycline-based chemotherapy in the BREAKFAST trial and in an independent retrospective control cohort of n=33 patients with TNBC treated with neoadjuvant anthracycline-containing chemotherapy alone. Each boxplot indicates the 25th and 75th percentiles of the distribution, while the horizontal line inside the box indicates median values. Dots indicate individual values. P values are referred to the results of paired **(A, B)** and unpaired **(C)** Wilcoxon test. **(D)** Bar plots indicate the absolute number of patients (y-axis) who completed the number of FMD cycles indicated on the x-axis. **(E)** Pie-chart illustrating patient compliance, expressed as the

proportion of patient who were fully compliant during all the FMD cycles, or who underwent at least minor or major deviations during at least one FMD cycle (upper panel), or the percentage of total FMD cycles completed with minor, major, or no deviations (full compliance) from the prescribed scheme (lower panel). *FMD: Fasting-mimicking diet; LVEF: Left Ventricle Ejection Fraction; TNBC: Triple Negative Breast Cancer*.

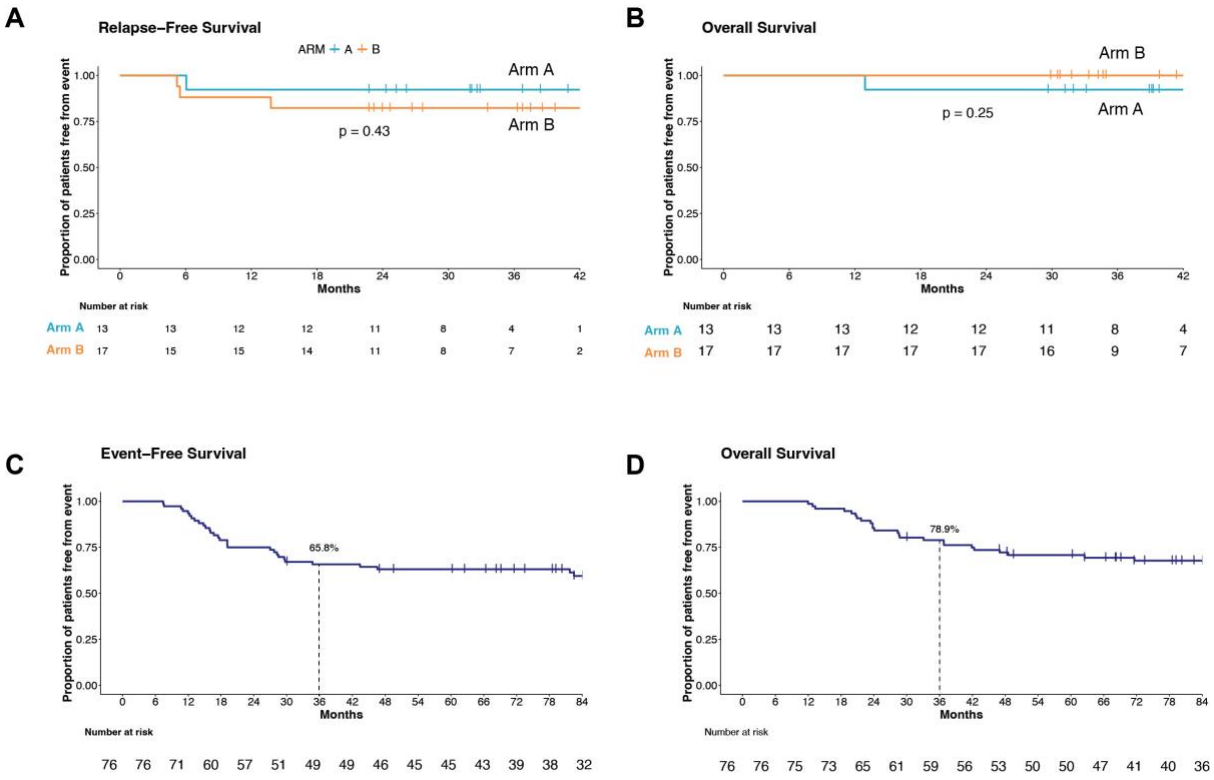

Figure S3, related to Figure 2. Relapse-Free Survival and Overall Survival. Kaplan Meier curves representing **(A)** RFS and **(B)** OS according to treatment arm in patients enrolled in the BREAKFAST trial. **(C)** EFS and **(D)** OS in an independent control cohort of patients with TNBC (n=76) treated with anthracycline-taxane based neoadjuvant chemotherapy at our Institution. Tick marks represent data censored at the last time that the patient was alive and without an event. P value of the log rank test is reported. *RFS: Relapse-Free Survival; EFS: Event-Free Survival; OS: Overall Survival.*

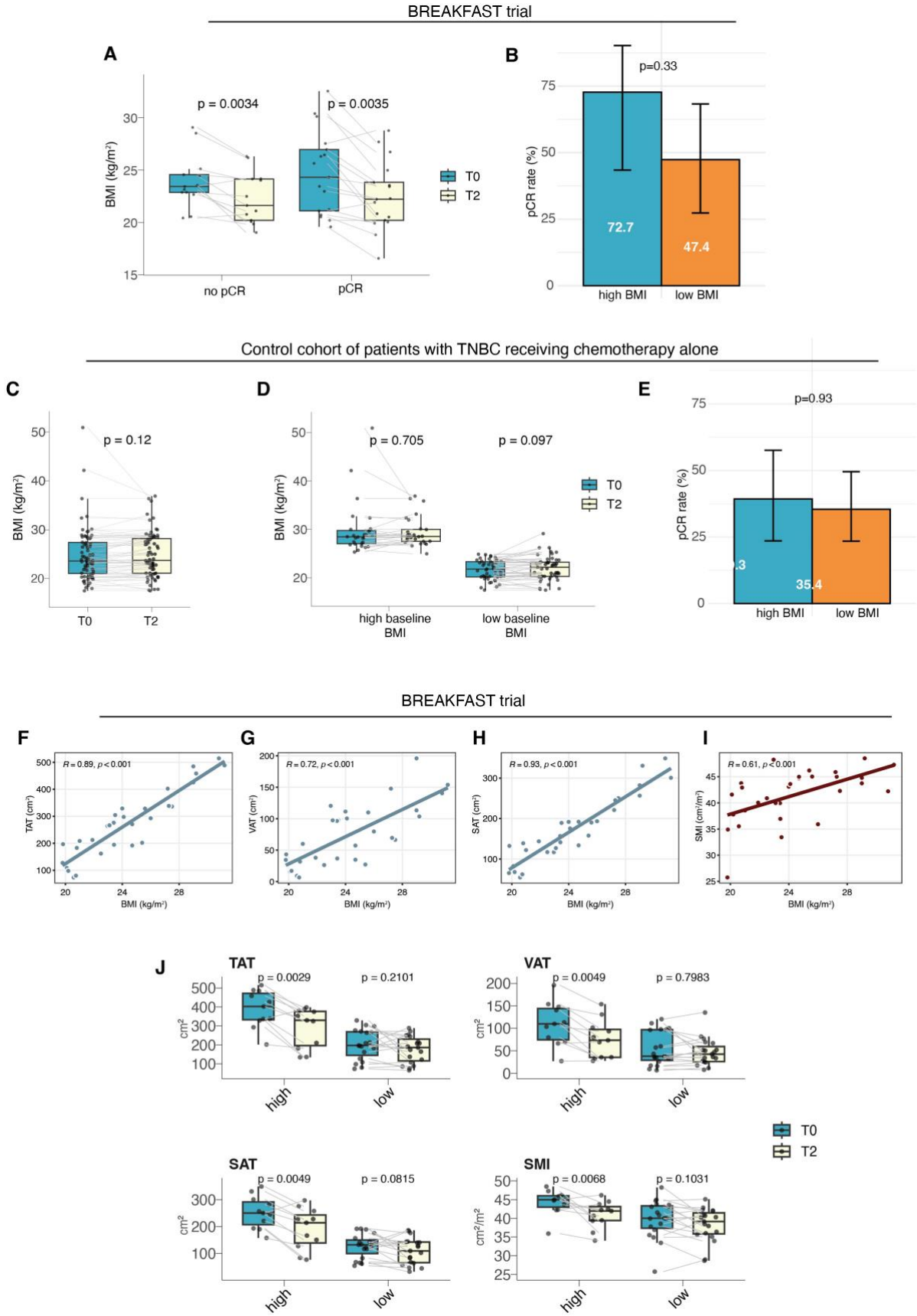

Figure S4, related to Figure 3. BMI according to pCR status and correlation with body composition

parameters. (A) BMI changes during the experimental treatment, according to pCR status. Patient BMI was calculated in the whole patient cohort (n=30) before treatment initiation (T0) and before surgery (T2). **(B)** pCR rates according to baseline BMI (low: <25 kg/m^2; high: ≥ 25 kg/m^2) in the BREAKFAST trial; **(C** and **D)** BMI changes during neoadjuvant chemotherapy in an independent retrospective control cohort of n=76 patients with TNBC treated with chemotherapy alone in our Institution (INT 92/20 cohort), evaluated **(C)** in the whole patient population and **(D)** according to baseline BMI (low: < 25 kg/m^2; high: ≥ 25 kg/m^2). Patient BMI was calculated before treatment initiation (T0) and before surgery (T2). **(E)** pCR rates according to baseline BMI (low: <25 kg/m^2; high: ≥25 kg/m^2) in the INT 92/20 cohort. **(F-I)** Spearman linear correlation of BMI and each of the indicated body composition parameters (TAT, VAT, SAT, SMI) in patients enrolled in the BREAKFAST trial (n=30). **(J)** Boxplots representing body composition parameters measured in matched CT scans performed at baseline (T0) and before surgery (T2) in n=30 patients, according to baseline BMI ("low": < 25 kg/m^2; n=19 patients; "high": ≥ 25 kg/m^2; n =11 patients). Each box plot indicates the 25th and 75th percentiles of the distribution of each body composition parameter, while the horizontal line inside the box indicates the median value of the distribution. Dots indicate parameter values of individual patients. P values refer to the paired Wilcoxon test. *BMI: Body Mass Index; SAT: Subcutaneous Adipose Tissue; SMI: Skeletal Muscle Index; TAT: Total Adipose Tissue; TNBC: Triple Negative Breast Cancer; VAT: Visceral Adipose Tissue.*

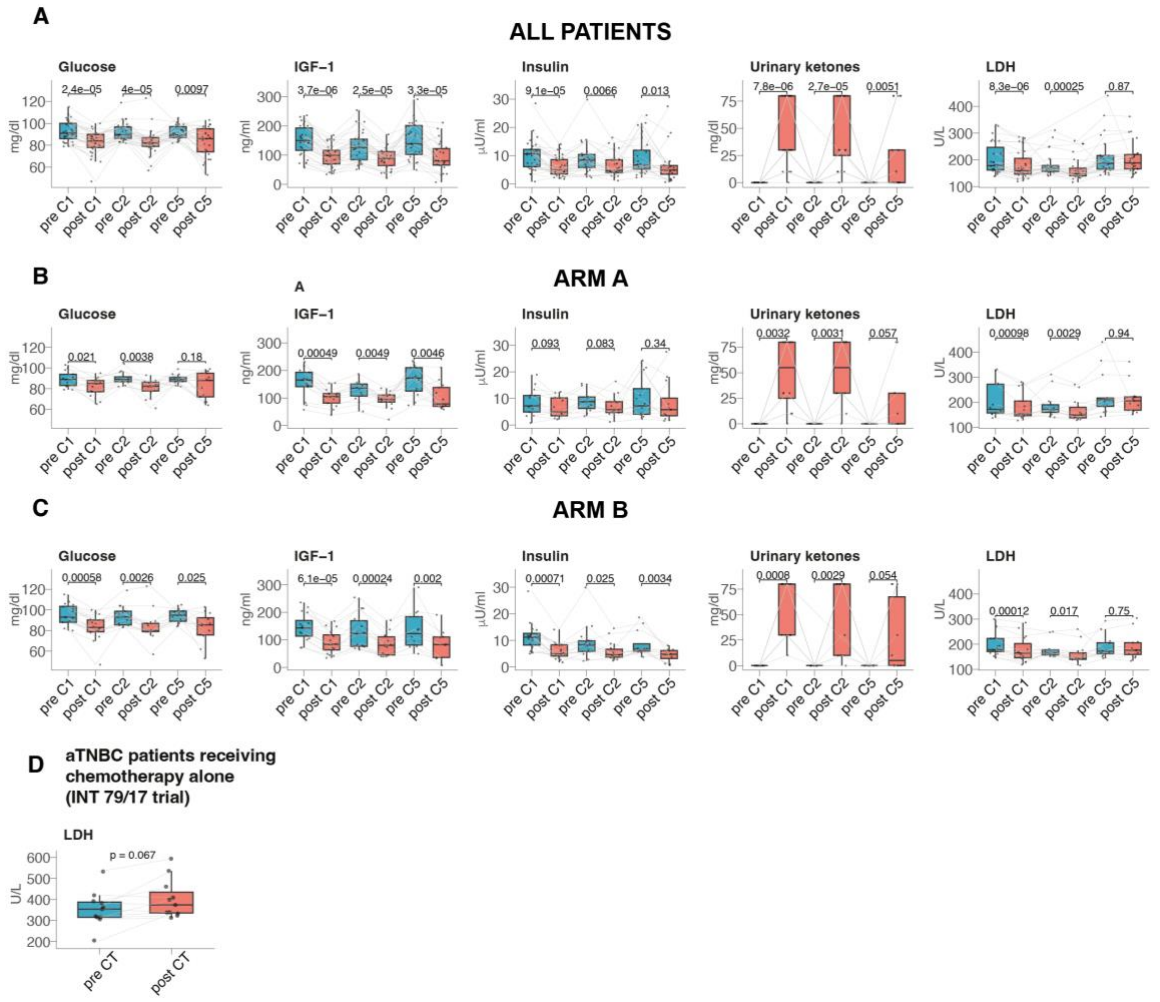

Figure S5, related to Figure 4. Changes in plasmatic and urine metabolites during the study treatment. (A-C) Concentration of blood glucose, insulin, IGF-1, LDH and urinary ketones measured before ("pre") and after ("post") the indicated FMD cycles, as well as at surgery: **(A)** in the whole patient cohort (n=29 matched samples; n=26 for LDH) of patients enrolled in the trial; (**B)** in patients randomized to arm A; (**C)** in patients randomized to arm B. **(D)** Blood LDH values before and after chemotherapy administration in a control cohort of n=13 patients with aTNBC receiving chemotherapy without the FMD in the context of an observational, prospective study (INT 79/17). Each boxplot indicates the 25th and 75th percentiles of the distribution of each blood parameter, while the horizontal line inside the box indicates the median values. Dots indicate individual parameter values. P values are obtained by paired Wilcoxon test. *aTNBC: advanced Triple Negative Breast Cancer; FMD: Fasting-mimicking diet; IGF-1 Insulin-like growth factor 1; LDH Lactate Dehydrogenase.*

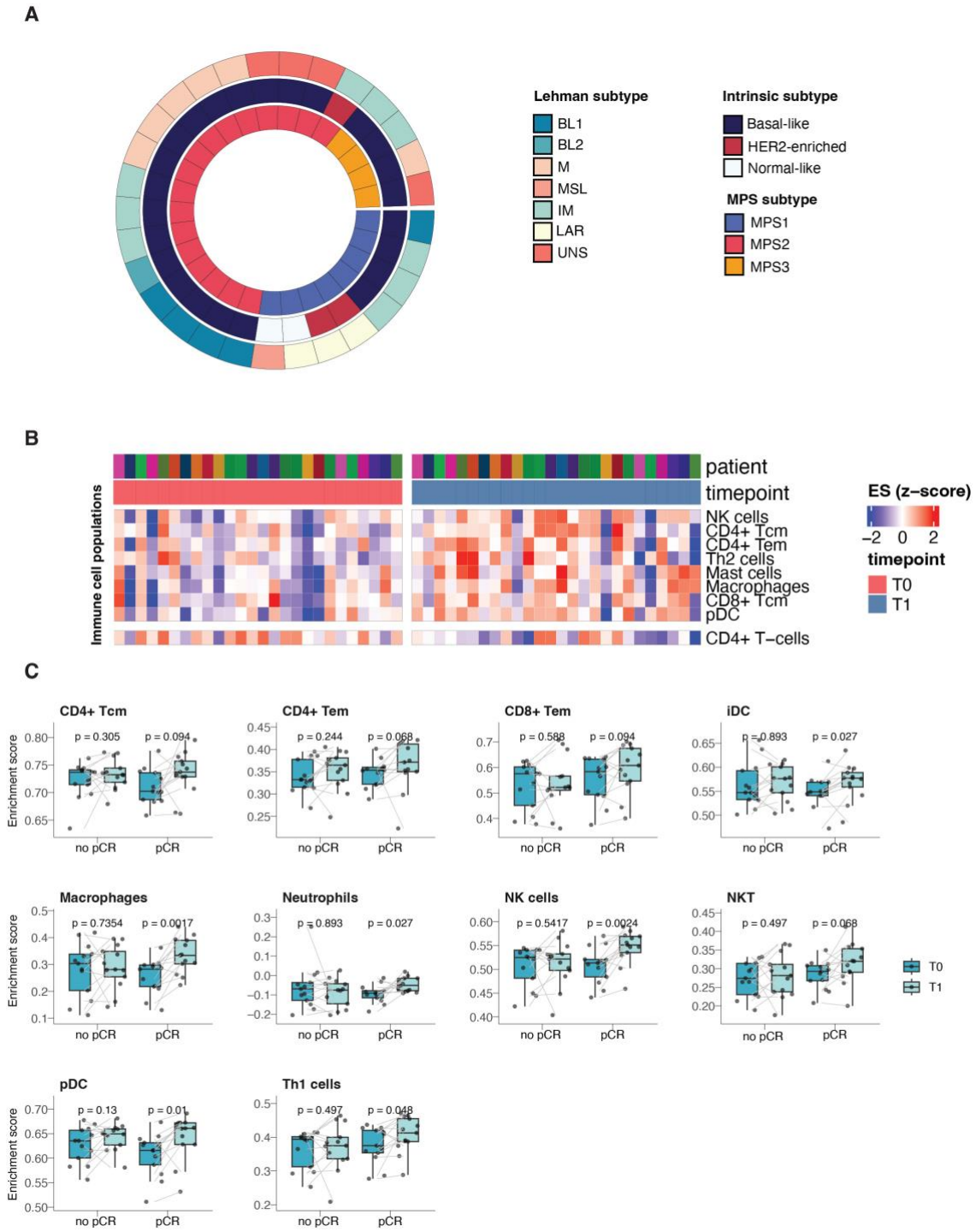

Figure S6, related to Figure 4. Modulation of intratumor immunity during experimental treatment. (A) "Lehmann" (outer circle), "Intrinsic subtype" (middle circle) and "metabolic classification" (inner circle) of individual baseline tumor specimen from patients enrolled in the BREAKFAST trial (n=29). **(B)** Heat map representing scores of leukocyte populations (Charoentong signatures) that were significantly modulated (Wilcoxon test $P < 0.05$) in T1 vs. T0 samples. **(C)** Boxplots representing scores of selected leukocyte populations

at T0 and T1, and according to pCR status. Each box plot indicates the 25th and 75th percentiles of the distribution of the variable, while the horizontal line inside the box indicates the median values. Dots indicate values of the indicated variable referring to individual patien. P values are obtained by paired Wilcoxon test. *cm: central memory, em: effector memory; ES: Enrichment Score; iDC: Interstitial Dendritic Cells; NK: natural killer, pCR: pathologic complete response; pDC: plasmacytoid dendritic cells.*

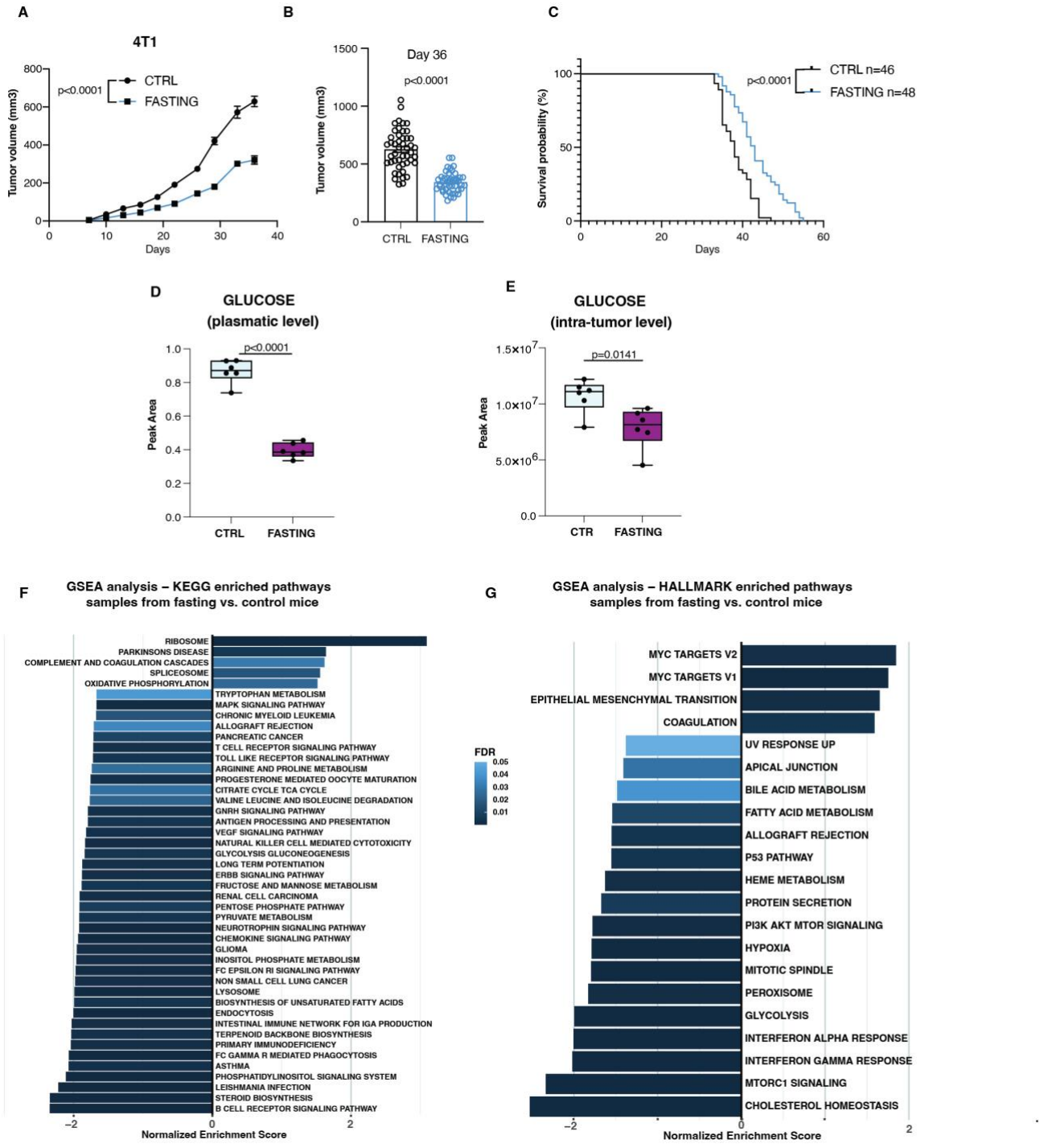

Figure S7, related to Figure 4. Modulation of intratumor glucose metabolism in a syngeneic TNBC mouse model. (A) Growth of 4T1-luc (constitutively expressing luciferase) cell transplants in the mammary fat pad of 7-weeks old female BALB/c mice fed with standard diet (control, or CTRL) or cyclic fasting (48-hours of water-only fasting, followed by ad libitum refeeding, and repeated every 7 days) (n=46 and n=48 mice, respectively). **(B)** Tumor volumes at day 36 are reported. **(C)** Survival curves of mice treated as described in (A) are reported.

Comparison of survival curves in CTRL vs. fasting arm was performed with Log-rank (Mantel-Cox) test. P values ≤ 0.05 were considered significant. Data from different (n=4) experiments with the same design were put together to generate curves in A, B and C. (**D** and **E**) Peak area of plasmatic (D) and intratumor (E) glucose levels measured in 4T1-bearing BALB/c mice through metabolomics analysis. Data are represented as mean ± SEM. P values were determined by unpaired t-test. **(F-G)** Gene set enrichment analysis (GSEA) using KEGG **(F)** and HALLMARK **(G)** gene sets, performed on genes ranked after differential expression analysis comparing mice treated with fasting (n = 6) and controls (n = 5, receiving ad libitum diet). Positive enrichment scores indicate upregulation in the fasting group, while negative scores indicate downregulation. The top 40 up- and down-regulated pathways, or all pathways with false discovery rate <0.05 (if less than 40 pathways are deregulated) are shown.

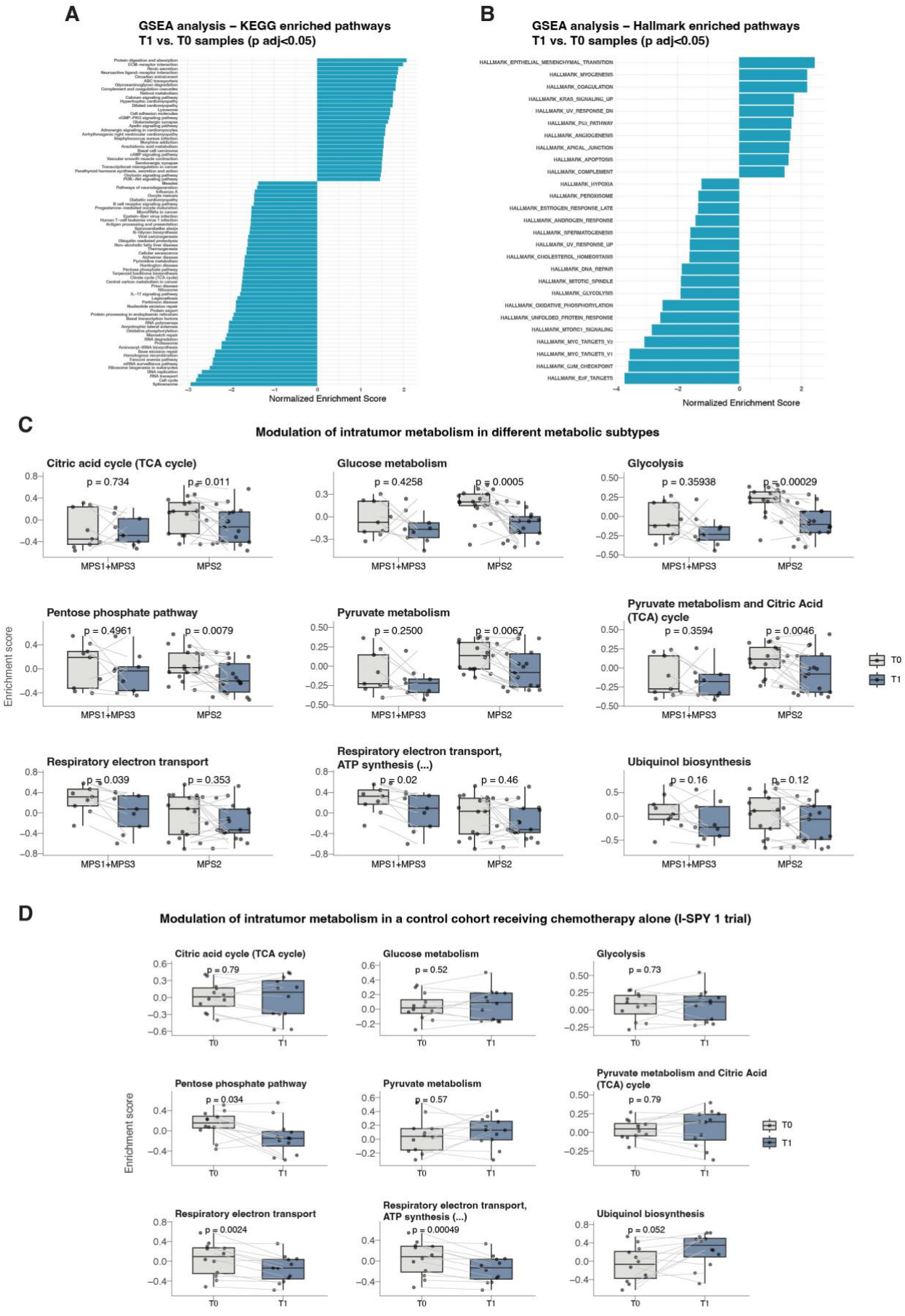
A
GSEA analysis – KEGG enriched pathways
T1 vs. T0 samples (p adj<0.05)
Normalized Enrichment Score
B
GSEA analysis – Hallmark enriched pathways
T1 vs. T0 samples (p adj<0.05)
HALLMARK_EPITHELIAL_MESENCHYMAL_TRANSITION
HALLMARK_MYOGENESIS
HALLMARK_COAGULATION
HALLMARK_KRAS_SIGNALING_UP
HALLMARK_UV_RESPONSE_DN
HALLMARK_P53_PATHWAY
HALLMARK_ANGIOGENESIS
HALLMARK_APICAL_JUNCTION
HALLMARK_APOPTOSIS
HALLMARK_COMPLEMENT
HALLMARK_HYPOXIA
HALLMARK_PEROXISOME
HALLMARK_ESTROGEN_RESPONSE_LATE
HALLMARK_ANDROGEN_RESPONSE
HALLMARK_SPERMATOGENESIS
HALLMARK_UV_RESPONSE_UP
HALLMARK_CHOLESTEROL_HOMEOSTASIS
HALLMARK_DNA_REPAIR
HALLMARK_MITOTIC_SPINDLE
HALLMARK_GLYCOLYSIS
HALLMARK_OXIDATIVE_PHOSPHORYLATION
HALLMARK_UNFOLDED_PROTEIN_RESPONSE
HALLMARK_MTORC1_SIGNALING
HALLMARK_MYC_TARGETS_V2
HALLMARK_MYC_TARGETS_V1
HALLMARK_G2M_CHECKPOINT
HALLMARK_E2F_TARGETS
Normalized Enrichment Score
C
Modulation of intratumor metabolism in different metabolic subtypes
Citric acid cycle (TCA cycle)
p = 0.734
p = 0.011
Glucose metabolism
p = 0.4258
p = 0.0005
Glycolysis
p = 0.35938
p = 0.00029
Pentose phosphate pathway
p = 0.4961
p = 0.0079
Pyruvate metabolism
p = 0.2500
p = 0.0067
Pyruvate metabolism and Citric Acid (TCA) cycle
p = 0.3594
p = 0.0046
Respiratory electron transport
p = 0.039
p = 0.353
Respiratory electron transport, ATP synthesis (...)
p = 0.02
p = 0.46
Ubiquinol biosynthesis
p = 0.16
p = 0.12
Enrichment score
MPS1+MPS3
MPS2
T0
T1
D
Modulation of intratumor metabolism in a control cohort receiving chemotherapy alone (I-SPY 1 trial)
Citric acid cycle (TCA cycle)
p = 0.79
Glucose metabolism
p = 0.52
Glycolysis
p = 0.73
Pentose phosphate pathway
p = 0.034
Pyruvate metabolism
p = 0.57
Pyruvate metabolism and Citric Acid (TCA) cycle
p = 0.79
Respiratory electron transport
p = 0.0024
Respiratory electron transport, ATP synthesis (...)
p = 0.00049
Ubiquinol biosynthesis
p = 0.052
Enrichment score
T0
T1

Figure S8, related to Figure 4. Modulation of intratumor glucose metabolism and OXPHOS pathways according to metabolic subtype. (A and **B)** Bar plots representing KEGG **(A)** and Hallmark **(B)** pathways that are significantly (FDR < 0.05) enriched by GSEA in T1 vs. T0 tumor specimens. Each bar represents the NES. **(C)** Boxplots representing GSVA ESs of Reactome metabolic pathways related to glucose metabolism and OXPHOS in n=26 matched tumor samples collected at T0 and T1, and according to metabolic classification, in the BREAKFAST trial. **(D)** Boxplots representing GSVA ESs of Reactome metabolic pathways related to glucose metabolism and OXPHOS in n=12 matched tumor samples collected before (T0) and after (T1) one cycle of treatment in a cohort of patients with early-stage TNBC receiving neoadjuvant chemotherapy alone (I-SPY1 trial). Each box plot indicates the 25^{th} and 75^{th} percentiles of the distribution of ES, while the horizontal line inside the box indicates the median values. Dots indicate individual ES values. P values are obtained by paired Wilcoxon test. *ES: Enrichment Score; GSEA: Gene Set Enrichment Analysis; GSVA: Gene Set Variation Analysis; NES: Normalized Enrichment Score.*

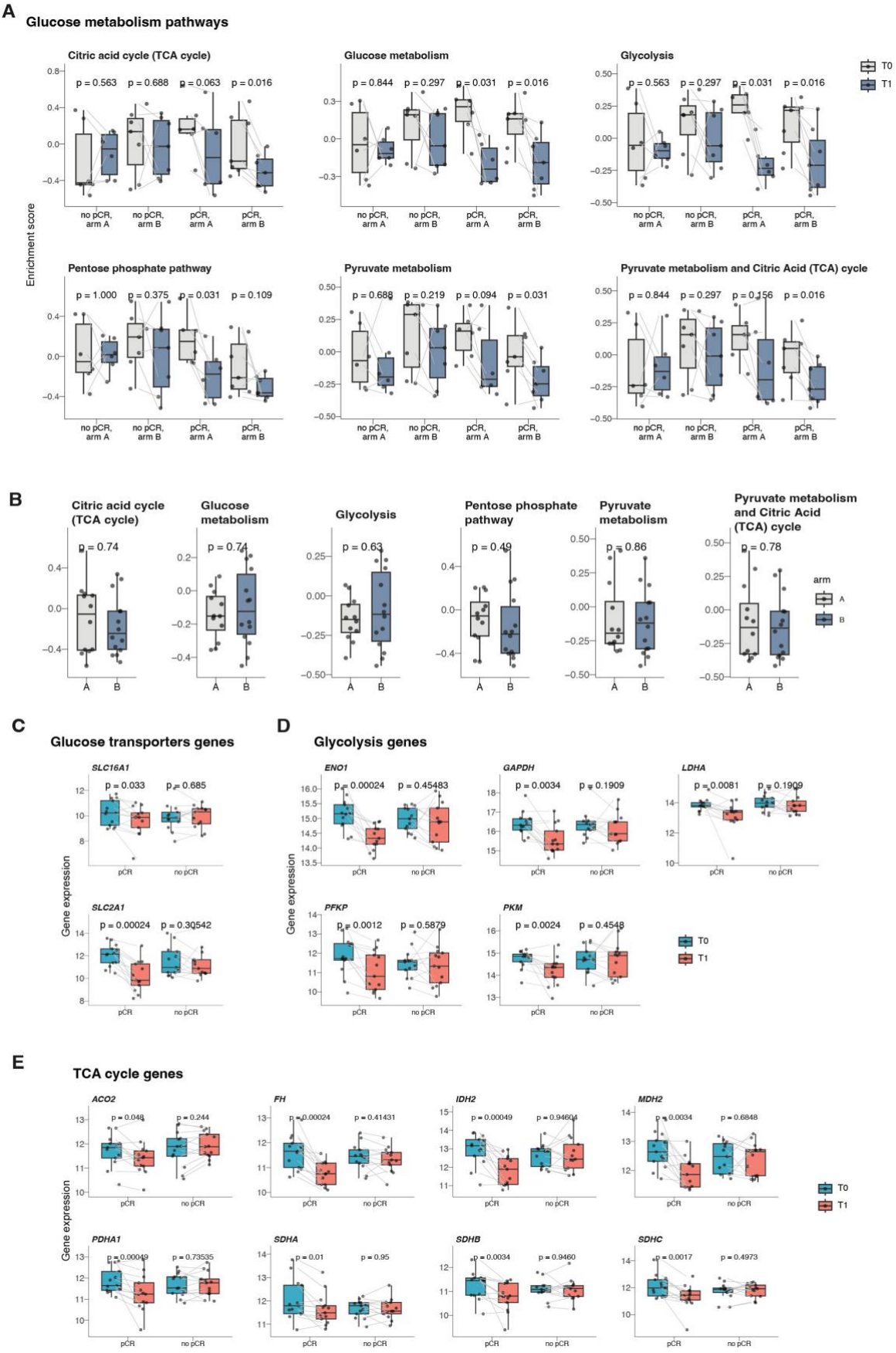

Figure S9, related to Figure 5. Modulation of intratumor glucose and pyruvate metabolism pathways or

genes according to pCR and treatment arm. (A) Boxplots representing GSVA ESs of selected Reactome pathways in n=26 matched tumor samples collected at T0 and at T1, and according to pCR status and treatment arm. **(B)** Boxplots representing GSVA ESs of selected Reactome pathways in n=26 tumor samples collected at T1 according to treatment arm. **(C-E)** Boxplots representing the expression of gene transcripts involved in **(C)** glucose/lactate transport, **(D)** glycolysis and **(E)** TCA cycle in n=26 matched tumor samples collected at T0 and T1 and according to pCR status. Each box plot indicates the 25^{th} and 75^{th} percentiles of the distribution of the variable, while the horizontal line inside the box indicates the median values. Dots indicate individual variable values. P values are obtained by paired Wilcoxon test. *ES: Enrichment Score; GSVA: Gene Set Variation Analysis; pCR: pathologic complete response.*

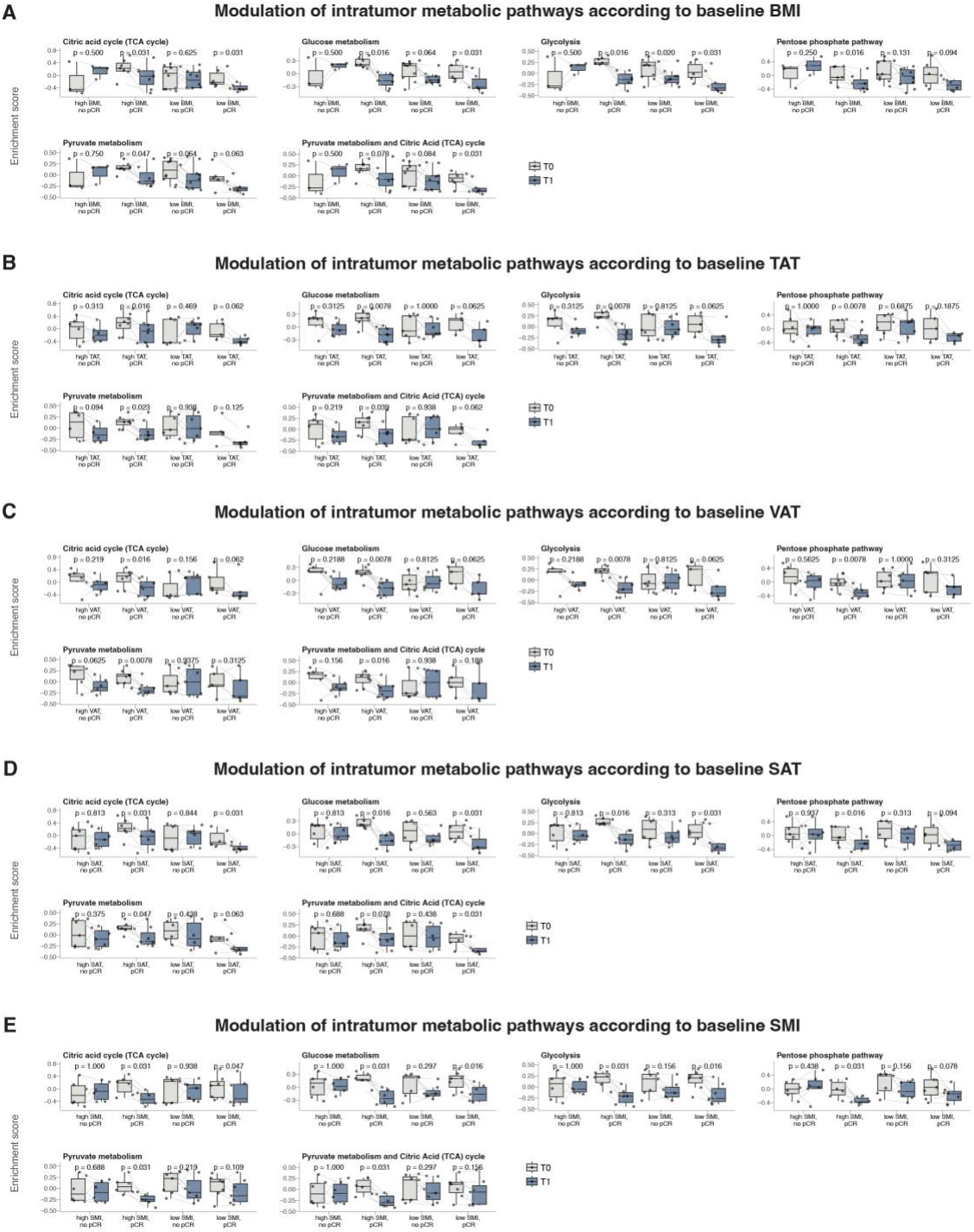

Figure S10, related to Figure 5. Modulation of intratumor glucose, pyruvate and TCA cycle metabolism according to pCR and BMI/body composition parameters. (A-E) Boxplots representing GSVA ESs of selected Reactome pathways in n=26 matched tumor samples collected at T0 and at T1 and according to both pCR status and: (A) baseline BMI, (B) baseline TAT, (C) baseline VAT, (D) baseline SAT, (E) baseline SMI. Each box plot indicates the 25th and 75th percentiles of the ES distribution, while the horizontal line inside the box indicates the median values. Dots indicate individual ES values. P values are obtained by paired Wilcoxon test. BMI: Body

Mass Index; *ES: Enrichment Score; GSVA: Gene Set Variation Analysis; pCR: pathologic complete response; SAT: Subcutaneous Adipose Tissue; SMI: Skeletal Muscle Index. TAT: Total Adipose Tissue; VAT: Visceral Adipose Tissue*.

Table S1 related to Table 1. Treatment-related adverse events

Adverse event	Overall (n= 30)		Arm A (n = 13)		Arm B (n = 17)	
	Any grade	G3-G4	Any grade	G3-G4	Any grade	G3-G4
Fatigue	29 (97%)	1 (3%)	12 (92%)	1 (8%)	17 (100%)	0 (0%)
FMD-related	22 (73%)	1 (3%)	10 (77%)	1 (8%)	2 (71%)	0 (0%)
Nausea	30 (100%)	2 (7%)	13 (100%)	0 (0%)	17 (100%)	2 (12%)
FMD-related	17 (57%)	0 (0%)	6 (46%)	0 (0%)	11 (65%)	0 (0%)
Diarrhea	16 (53%)	2 (7%)	4 (31%)	2 (15%)	12 (71%)	0 (0%)
FMD-related	0 (0%)	0 (0%)	0 (0%)	0 (0%)	0 (0%)	0 (0%)
Stomatitis	15 (50%)	0 (0%)	6 (46%)	0 (0%)	9 (53%)	0 (0%)
FMD-related	0 (0%)	0 (0%)	0 (0%)	0 (0%)	0 (0%)	0 (0%)
Peripheral neuropathy	13 (43%)	0 (0%)	5 (38%)	0 (0%)	8 (47%)	0 (0%)
FMD-related	0 (0%)	0 (0%)	0 (0%)	0 (0%)	0 (0%)	0 (0%)
Headache	13 (43%)	0 (0%)	6 (46%)	0 (0%)	7 (41%)	0 (0%)
FMD-related	7 (23%)	0 (0%)	3 (23%)	0 (0%)	4 (24%)	0 (0%)
Fever	12 (40%)	0 (0%)	5 (38%)	0 (0%)	7 (41%)	0 (0%)
FMD-related	0 (0%)	0 (0%)	0 (0%)	0 (0%)	0 (0%)	0 (0%)
Vomit	10 (33%)	0 (0%)	6 (46%)	4 (24%)	0 (0%)	0 (0%)
FMD-related	1 (3%)	0 (0%)	0 (0%)	1 (6%)	0 (0%)	0 (0%)
GI pain	10 (33%)	0 (0%)	0 (0%)	4 (31%)	6 (35%)	0 (0%)
FMD-related	2 (7%)	0 (0%)	0 (0%)	0 (0%)	2 (12%)	0 (0%)
Constipation	9 (30%)	0 (0%)	3 (23%)	0 (0%)	6 (35%)	0 (0%)
FMD-related	5 (17%)	0 (0%)	2 (15%)	0 (0%)	3 (18%)	0 (0%)
Muscle cramps	8 (27%)	0 (0%)	3 (23%)	0 (0%)	5 (29%)	0 (0%)
FMD-related	0 (0%)	0 (0%)	0 (0%)	0 (0%)	0 (0%)	0 (0%)
Dizziness	6 (20%)	0 (0%)	2 (15%)	0 (0%)	4 (24%)	0 (0%)
FMD-related	5 (17%)	0 (0%)	1 (8%)	0 (0%)	4 (24%)	0 (0%)
Insomnia	6 (20%)	0 (0%)	2 (15%)	0 (0%)	4 (24%)	0 (0%)
FMD-related	2 (7%)	0 (0%)	1 (8%)	0 (0%)	1 (6%)	0 (0%)
Febrile neutropenia		3 (10%)		1 (8%)		2 (12%)
FMD-related		0 (0%)		0 (0%)		0 (0%)
Weight loss	20 (67%)	0 (0%)	7 (54%)	0 (0%)	13 (76%)	0 (0%)
FMD-related	20 (67%)	0 (0%)	7 (54%)	0 (0%)	13 (76%)	0 (0%)
Anemia	29 (97%)	5 (17%)	13 (100%)	2 (15%)	16 (94%)	3 (18%)
FMD-related	0 (0%)	0 (0%)	0 (0%)	0 (0%)	0 (0%)	0 (0%)
WBCs decrease	29 (97%)	13 (43%)	13 (100%)	5 (38%)	16 (94%)	8 (47%)
FMD-related	0 (0%)	0 (0%)	0 (0%)	0 (0%)	0 (0%)	0 (0%)
Neutropenia	28 (93%)	17 (57%)	13 (100%)	6 (46%)	15 (88%)	11 (65%)
FMD-related	0 (0%)	0 (0%)	0 (0%)	0 (0%)	0 (0%)	0 (0%)
ALT increase	18 (60%)	1 (3%)	7 (54%)	0 (0%)	11 (65%)	1 (6%)
FMD-related	2 (7%)	0 (0%)	1 (8%)	0 (0%)	1 (6%)	0 (%)
AST increase	17 (57%)	1 (3%)	9 (69%)	0 (0%)	8 (47%)	1 (6%)
FMD-related	1 (3%)	0 (0%)	0 (0%)	0 (0%)	1 (6%)	0 (0%)
Total cholesterol increase	17 (57%)	0 (0%)	0 (0%)	7 (54%)	10 (59%)	0 (0%)
FMD-related	13 (43%)	0 (0%)	0 (0%)	6 (46%)	7 (41%)	0 (0%)
Uricemia increase	8 (27%)	0 (0%)	2 (15%)	0 (0%)	6 (35%)	0 (0%)
FMD-related	5 (17%)	0 (0%)	1 (8%)	0 (0%)	4 (24%)	0 (0%)
Hypertriglyceridemia	7 (23%)	0 (0%)	4 (31%)	0 (0%)	3 (18%)	0 (0%)
FMD-related	7 (23%)	0 (0%)	4 (31%)	0 (0%)	3 (18%)	0 (0%)
Thrombocytopenia	2 (7%)	1 (3%)	0 (0%)	0 (0%)	2 (12%)	1 (6%)
FMD-related	0 (0%)	0 (0%)	0 (0%)	0 (0%)	0 (0%)	0 (0%)
Hypoglycemia	7 (23%)	0 (0%)	5 (38%)	0 (0%)	2 (12%)	0 (0%)
FMD-related	7 (23%)	0 (0%)	5 (38%)	0 (0%)	2 (12%)	0 (0%)
SAEs		2 (7%)		0 (0%)		2 (12%)
FMD-related		0 (0%)		0 (0%)		0 (0%)
Any AEs	30 (100%)	21 (70%)	13 (100%)	7 (54%)	17 (100%)	14 (82%)
FMD-related	30 (100%)	1 (3%)	13 (100%)	1 (8%)	17 (100%)	0 (0%)

Abbreviations: AEs: adverse events; ALT Alanine transaminase; AST Aspartate transaminase; FMD: Fasting-mimicking diet; GI: gastrointestinal; SAEs: serious adverse events; WBCs: White blood cells.

130
131 **Table S2, related to Figure 2. Published phase II and III studies with neoadjuvant anthracycline plus taxanes in TNBC**
132

Study	Type of study	Primary endpoint	Secondary endpoints	Regimen#	N of pts with TNBC #	pCR rate[i#]	Age (median)	cT1-2 (n (%))	cN0 (n (%))	stage I-II (n (%))	ECOG PS0 (n (%))	Premenopausal (n (%))
GEICAM/2006-03[a]	Phase II	ypT0/is	ypT0/is pN0, clinical response rate, safety	EC (90/600 mg/m^2) Q3W for 4 cycles → Docetaxel 100 mg/m^2 Q3W for 4 cycles	46	30%[j]	47 y	37 (81%)	21 (46%)	na	38 (83%)	33 (72%)
GeparSixto GBG66[b]	Phase II	ypT0pN0	ypT0/is pN0, clinical response rate, safety	Paclitaxel 80 mg/m^2 weekly + non-pegylated liposomal doxorubicin 20 mg/m^2 weekly + Bevacizumab 15 mg/kg Q3W for 18 wks	157	42.7%[j]	47 y*	264 (91%)*	160 (57%)*	na	na	na
CALGB 40603 Alliance[c]	Phase II	ypT0/is	ypT0/is pN0, safety, RFS and OS	Paclitaxel 80 mg/m^2 weekly for 12 cycles→ ddAC (60/600 mg/m^2 Q2W) for 4 cycles	107	39%[j]	21%<40y, 59% 40-59y	78%	45%	na	69%	na
UMIN000003355[d]	Phase II	ypT0/is pN0	Clinical response rate, safety, DFS	Paclitaxel 80 mg/m^2 weekly for 12 cycles→ CEF (500/100/500 mg/m^2) Q3W for 4 cycles	38	26.3 %	47 y*	67 (73.6%)*	30 (33%)*	75 (82.5%)*	91 (100%)*	54 (59.3%)*
NCT01276769[e]	Phase II	ypT0/is pN0	ORR, RFS, OS, safety	Epirubicin 75 mg/m^2 + Paclitaxel 175 mg/m^2 Q3W for 4-6 cycles	43	14%	46 y	29 (65.9%)	8 (18.18%)	15 (34.09%)	na	30 (68.2%)
GeparOcto GBG84[f]	Phase III	ypT0/is pN0	Toxicity, DFS, OS	iddEPC (150/ 225/2000 mg/m^2 Q2W)	200	48.5 %	48 y*	428 (92.6)*	249 (54.4)*	na	na	288 (61.3)*
BrighTNess[g]	Phase III	ypT0/is pN0	Clinical response rate, toxicity, EFS, OS	Paclitaxel 80 mg/m2 weekly for 12 cycles → ddAC or AC for 4 cycles	158	31%	51% < 50y	132 (84%)	94 (60%)	na	na	na
INT 92/20	Retrospective	ypT0/is pN0	DFS, OS	AT (60/200 mg/m^2 Q3W → CMF (600 40/600 mg/m^2 D1,8q28) for 3-4 cycles	76	37%	45 y	53 (69.3%)	29 (38%)	54 (71%)	na	na

Abbreviations: pCR: pathologic complete response, EC: Epirubicin plus Cyclophosphamide; AC: Adriamycin plus Cyclophosphamide; ddAC: dose-dense AC; CEF: Cyclophosphamide plus Epirubicin plus 5-Fluorouracil; iddEPC intense dose-dense Epirubicin plus Paclitaxel plus Cyclophosphamide; AT:doxorubicin plus paclitaxel; CMF: cyclophosphamide plus methotrexate plus 5-Fluorouracil; Q3W: every 3 weeks; Q2W: every 2 weeks.
*A Alba et al, Breast Cancer Res Treat 2012; b Von Minckwitz et al, Lancet Oncol 2014; c Sikov et al, J Clin Oncol, 2015; d Ando et al, Breast Cancer Res Treat 2014; e Zhang et al, Oncotarget 2016; f Schneeweiss et al, Eur J Cancer 2019; gLoibl et al Lancet Oncol 2018;h INT92/20: cohort of n=76 patients with TNBC treated at our Institution with neoadjuvant anthracycline/taxane based chemotherapy. iThe percentage refers to pCR rates in anthracycline plus taxanes treated patients. In studies enrolling different breast cancer subtypes, the percentage refers to pCR rates in the TNBC subgroup. jpCR rate always refers to the rate ypT0/is pN0, also if not the primary study endpoint. *data of the overall population, as data for TNBC subgroup are not reported #in trials with multiple arms, data refers to the anthracycline plus taxanes based chemotherapy arm*

133
134

Table S3, related to Figure 2. Characteristics of patients with TNBC enrolled in the observational INT 92/20 trial included in the present analysis

Characteristic		Whole patient cohort (n = 76)	Patients with available LVEF evaluation (*N = 33*)	p
Age	Median (IQR)	46 (41, 57)	44 (39, 57)	0.6[d]
Primary tumor[a]				0.9
	1	4 (5.3%)	3 (9.1%)	
	2	49 (65%)	21 (64%)	
	3	10 (13%)	4 (12%)	
	4	12 (16%)	5 (15%)	
Nodal status				0.4
	0	29 (38%)	17 (52%)	
	1	41 (54%)	14 (42%)	
	2	4 (5.3%)	0 (0%)	
	3	2 (2.6%)	2 (6.1%)	
Ki67[b]		60 (30, 80)	80 (60, 80)	0.037[d]
Grade[c]				0.8
	2	12 (17%)	4 (13%)	
	3	57 (83%)	28 (88%)	
BMI	Median (IQR)	23.5 (20.9, 27.4)	24.4 (22.2, 28.3)	0.4[d]

Data are presented as n (%) except where otherwise noted. The p value of the Pearson's chi squared test is indicated in the right column of the table, except where otherwise noted. The p value of the test is indicated in bold numbers when statistically significant. p-values were calculated excluding unknown values. [a] *data not available for 1 patient;* [b] *data not available for 4 patients,* [c] *data not available for 7 and 1 patients, respectively.* [d] *Wilcoxon rank sum test. Abbreviations: BMI: body mass index; IQR: Interquartile range.*

Additional supplemental information:

- **Methods S1 - Study protocol, related to STAR Methods**
- **Data S1 - Source Data related to Figures 2-6, S2-S10.**